ASTRONAUTICS RESEARCH REPORT
NO. 77-2

(NASA-CR-149885) WATER SPRAYS IN SPACE RETRIEVAL OPERATIONS (Pennsylvania State Univ.) 68 p HC A04/MF A01 CSCL 22A
N77-20128
Unclas
G3/13 21653

WATER SPRAYS IN SPACE RETRIEVAL OPERATIONS

BY
DOUGLAS C. FREESLAND
PROJECT ASSISTANT

ASTRONAUTICS RESEARCH

THE PENNSYLVANIA STATE UNIVERSITY
Department of Aerospace Engineering
233 Hammond Building
University Park, Pennsylvania 16802

APRIL 1977

RESEARCH SUPPORTED BY NASA GRANT NSG-7078

ABSTRACT

Recent experiments involving liquid jets exhausting into a vacuum have led to significant conclusions regarding techniques for detumbling and despinning disabled spacecraft during retrieval operations. A fine water spray directed toward a tumbling or spinning object may quickly form ice over its surface. The added mass of water will absorb angular momentum and slow the vehicle. As this ice sublimes it carries momentum away with it. Thus, a complete detumble or despin is possible by simply spraying water at a disabled vehicle. Experiments were conducted in a ground based vacuum chamber to determine physical properties of water-ice in a space-like environment. Additional ices, alcohol and ammonia, were also studied. An analytical analysis based on the conservation of angular momentum, resulted in despin performance parameters, i.e., total water mass requirements and despin times. The despin and retrieval of a disabled spacecraft was considered to illustrate a potential application of the water spray technique.

TABLE OF CONTENTS

LIST OF TABLES

LIST OF FIGURES

NOMENCLATURE

a	Surface Area, m^2
c.m.	Center of Mass
d	Nozzle Diameter, cm
$\vec{h}$	Angular Momentum Vector, N•m•s
I	Moment of Inertia, $N \cdot m \cdot s^2$
k	Coefficient of Accumulation
l	Distance Between the Nozzle and Impact Plate, cm
m	Mass, kg
r	Radial Distance from Axis of Rotation to Ice Element, m
ν	Sublimation Rate, $kg \cdot m^{-2} \cdot s^{-1}$
$\vec{\omega}$	Angular Velocity Vector, s^{-1}

<u>Subscripts</u>

f	Final
i	Initial
s	Satellite
t	Total
v	Vehicle
w	Water-Ice

ACKNOWLEDGMENTS

The author wishes to express his gratitude and appreciation to Dr. Marshall H. Kaplan, Associate Professor of Aerospace Engineering, for his help in the development of the problem and invaluable aid during the course of this work. The author also wishes to acknowledge the United States Air Force for the opportunity to conduct this research through an educational delay. The work reported here was supported by NASA Grant NSG-7078.

CHAPTER I

INTRODUCTION

With the advent of the space shuttle era retrieval of disabled spacecraft will become possible. Prior to any attempted retrieval, however, vehicle angular momentum must be nullified. A disabled spacecraft's angular momentum takes the form of either spinning or tumbling motion. This motion may be the result of a wildly firing thruster, collision with another vehicle, or loss of attitude control. Hard docking by a manned retrieval craft is not possible because of the hazardous environment to which the crew would be exposed. Furthermore, devices which might be used for capturing objects are not capable of grabbing something which is spinning or tumbling. There have been numerous techniques and hardware proposed to passivate, i.e , detumble or despin, a disabled vehicle. However, all of these devices represent complicated systems and are expensive and massive. A new technique involving liquid sprays has been conceived and appears to offer lower complexity, cost and mass.

1.1 Historical Development

Development of the water spray technique (WST) for space retrieval operations has arisen out of a need for a simple and inexpensive means of eliminating a disabled spacecraft's angular momentum. Additional design criteria are listed in Table I.

Early passivation schemes have included mechanical devices, nets, cables and rockets (1). Mechanical devices employ a synchronized, rotating, docking mechanism. Nets are envisioned as catching

Table I

Design Criteria for a Satellite Passivation Scheme (2)

1.	Low development costs
2.	Low recurring costs
3.	Available for operation at short notice
4.	Within shuttle orbiter payload capability
5.	Applicable to a wide range of vehicle sizes
6.	Should not damage tumbling spacecraft
7.	Operated easily without specialized crew
8.	High reliability
9.	Should pose no hazard to the retrieval spacecraft

and entangling the tumbling spacecraft, arresting its motion by the net's attachment to the rescue vehicle or by rockets of varying sophistication. Cables are shot out toward the tumbling spacecraft, "harpooning" it, wrapping themselves around it, or otherwise offering a means of providing a torque. Finally, rockets may be attached to the disabled vehicle to provide a detumbling or despinning torque. Each of these schemes have their drawbacks which do not satisfy the design criteria.

Recent proposals have included the use of water jets to provide an external torque to a tumbling or spinning spacecraft (3). The concept involves impinging momentum to eliminate angular momentum. Here again, a complex system is required since proper aiming and sequencing of the impinging water jet is necessary for a successful detumble. It was out of experimental investigation of this latter scheme that the WST was conceived.

Liquid jet experiments were carried out to investigate the properties of jets impinging upon surfaces in vacuum. During some of these experiments it was realized that water jets tend to form ice on an object downstream. This experimental accident led M.H. Kaplan, at The Pennsylvania State University, to the concept of using the ice advantageously (4).

1.2 Water Spray Technique

A new technique for eliminating angular momentum involves the use of liquids, such as water, in a spray technique. The idea is to spray water at a tumbling or spinning object such that the water tends to accumulate on the target and form ice as illustrated in Figure 1.

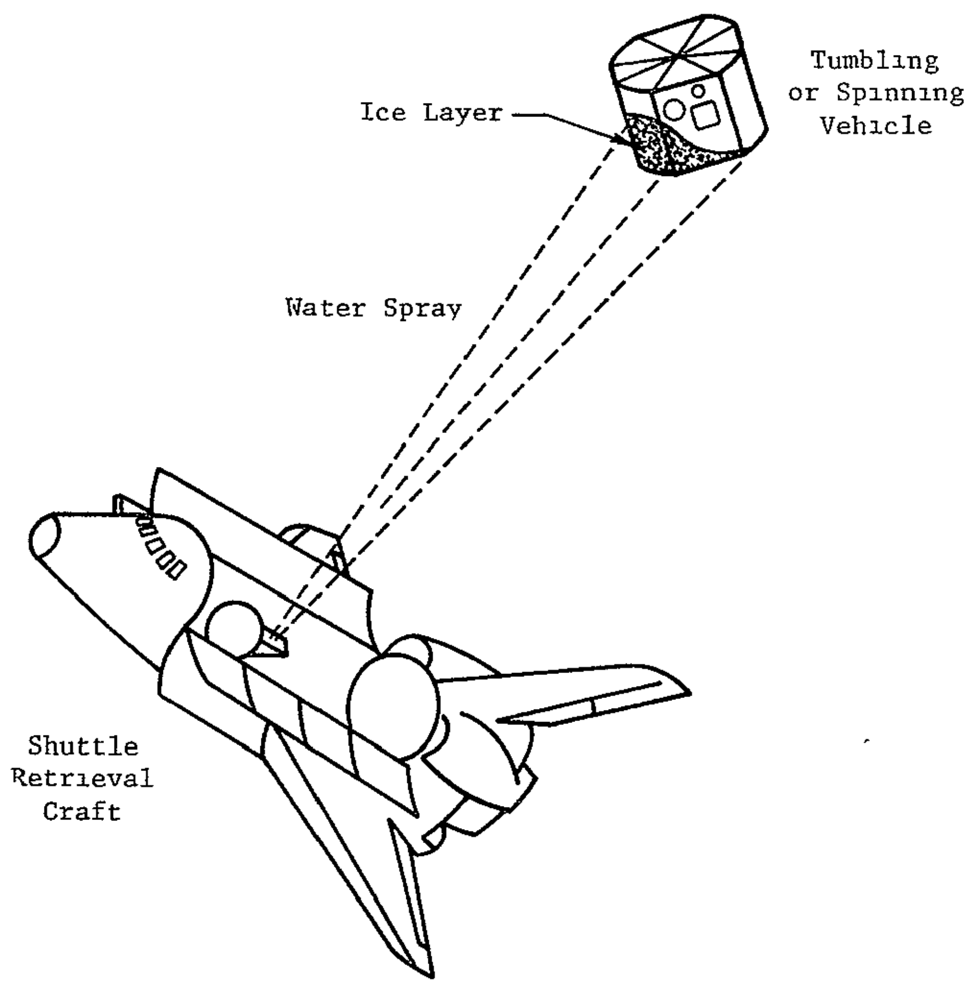

Figure 1 Water Spray Scheme

This formation of ice tends to absorb angular momentum. The concept has the obvious advantages of bypassing any hard docking requirements and being simple in application. Very little hardware or logic is required. The shuttle crew simply points a nozzle at an object, turns on a valve and waits for the object to despin or detumble. When a low enough angular rate is observed of the object, the shuttle manipulator can then capture it and place it in the shuttle or carry out the prescribed refurbishment.

1.3 Purpose and Objectives

It is the purpose of this investigation to examine the WST. A series of experiments have been conducted to determine physical properties of water sprays exhausting into a vacuum. A computer model is built which together with the experimental results, yields satellite despin performance parameters. To demonstrate an application of the WST, the selection and retrieval of an actual disabled spacecraft is considered.

CHAPTER II

PREVIOUS INVESTIGATIONS

The use of water sprays as a technique to eliminate angular momentum was first introduced at the 27th Congress of the International Astronautical Federation (5). A review of related work has revealed that the use of water sprays, as opposed to water jets, is a new and original technique for eliminating spacecraft angular momentum.

Other investigators have done experiments and analytical work related to sublimation rates of various substances in space. However, very few quantitative analyses have been performed dealing with the sublimation of ice in a hard vacuum. Two investigations were found to be related to this work. One is analytical and the other experimental.

Watson (6) performed analyses on various ices in heliocentric orbits. A simple energy balance was constructed across the surface of the ice from which the particle's lifetime was calculated as a function of its distance from the sun. Ices considered included water, ammonia, carbon dioxide and methane. The results are tabulated in Table II and indicate that water-ice has the longest lifetime while ammonia-ice sublimes about three times as fast. Carbon dioxide-ice and methane-ice sublime at a rate twelve times faster than water-ice. These results were obtained assuming that the ice particles were in circular heliocentric orbits at a distance of one astronomical unit from the sun. Effects related to the presence of the earth were not considered which resulted in lower energy absorbtion and sublimation rates and longer lifetimes of the ice spheres.

Table II

The Stability of 1 km Ice Spheres in Circular Heliocentric Orbits at a Solar Distance of One Astronomical Unit

Ice	Lifetime (years)
Water	530
Ammonia	167
Carbon Dioxide	42
Methane	42

By applying optical techniques to normal releases of water into space during Apollo lunar missions, Sharma (7) has determined size histories of micron size ice particles. This experiment determined that the radius of a particle of water-ice in a near earth orbit (650 km altitude) will decrease by a factor of 1/e in 1100 seconds, i.e., exponential folding time of 1100 seconds. For particles located at distances greater than 10 earth radii, where the equilibrium temperatures of the water-ice are so low that emission of radiation dominates sublimation and particle lifetimes increase considerably, the exponential folding time is 1.0×10^5 seconds. These results are listed in Table III. Since the shuttle will operate in a near earth environment and since the experimental results were from direct observation, an exponential folding time of 1100 seconds has been used in the analytical development of the WST.

Table III

Water-Ice Exponential Folding Times (7)

Cislunar Space	Near Earth (650 km Altitude)	
e-Folding Time (sec)	e-Folding Time (sec)	Uncertainty Range (sec)
1×10^5	1100	1200 - 200

CHAPTER III

EXPERIMENTS

Experiments were conducted to determine physical properties of water sprays in a space-like environment. Additive and dispersion effects were also considered. The results, although basically qualitative, support the conclusions of Watson (6) and Sharma (7).

3.1 Purpose and Objectives

A series of experiments were conducted in a small vacuum chamber to determine the physical properties of water sprays in a space-like environment. Physical properties of interest included the accumulation and sublimation rates of water-ice as well as the effect of ice layer thickness on sublimation rates. Several additional parameters were studied and include:

1. Dispersion effects, i.e., the ratio of impact cross-sectional area to nozzle cross-sectional area.
2. The effects of ammonia and alcohol as additives on the physical properties of the water spray.

3.2 Apparatus

The water spray experiments were conducted in a small vacuum facility at The Pennsylvania State University. The facility consisted of four main elements: chamber, pumps, pressure sensors and test stand.

The vacuum chamber used was a stainless steel cylindrical structure with a diameter of 0.97 m and length of 2.11 m, enclosing a volume of 1.56 m^3. It was equipped with three plexiglas viewing ports as well as a stainless steel end plate through which all electrical, mechanical and fluidic interfaces were made. The chamber was evacuated continuously by a 41 cm ringjet booster pump and a Stokes 412H mechanical vacuum pump. This combination of pumps is capable of producing pressures on the order of 10^{-4} torr.

Two types of pressure sensors were employed during the course of the experiments. The first was a Philips Gauge. This type of pressure sensor measures the ionization potential between a pair of electrodes, converting this into a pressure reading. The second type of pressure sensor used was a MKS Baratron. This device measured pressure directly, i.e., force per unit area.

The test stand mounted inside the chamber included a nozzle, impact plate and reference grid as illustrated in Figure 2. A stainless steel circular tube with inside diameter, $d = 5.54 \times 10^{-2}$ cm, was used as a nozzle. The nozzle end was cut perpendicular to the tube's axis of symmetry with a cross-sectional area of 2.41×10^{-3} cm^2. Water was supplied to the nozzle from a reservoir open to atmospheric pressure. The impact plate consisted of a rigid aluminum plate also positioned perpendicular to the nozzle's axis of symmetry. The plate was mounted on a moveable base which could be located a distance l, from 5.0 cm to 16.0 cm downstream of the nozzle. Aligned parallel to the nozzle's axis of symmetry, was the reference grid, an aluminum plate with a 0.64 cm grid etched on its surface.

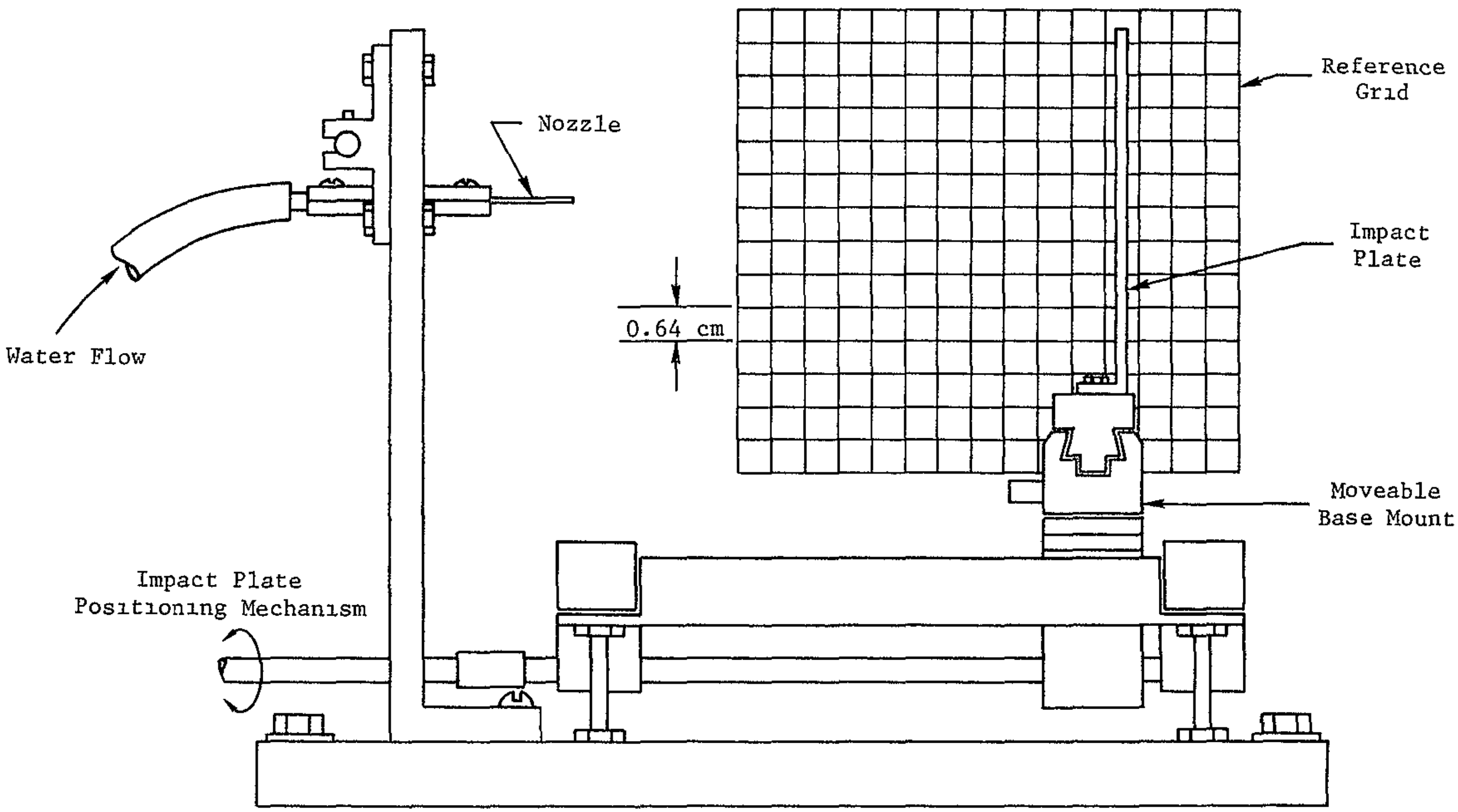

Figure 2. Experimental Test Stand

3.3 Procedure

In order to satisfy experimental purpose and objectives, numerous runs were made using water and concentrations of ammonia and alcohol. A typical run could be divided into four phases: pump down, ice accumulation, ice sublimation and pump up. Initially the vacuum chamber was at atmospheric pressure. Once the chamber was properly sealed, the mechanical and diffusion pumps were used to produce the vacuum. After several hours, the pressure in the chamber had reached a sufficiently low value, on the order of 10^{-4} torr. At this time a valve was quickly opened and closed allowing less than 0.005 liters of water to flow from the reservoir through the nozzle, impinging upon the impact plate as illustrated in Figure 3. Upon impact the water immediately froze, forming a thin layer of ice. As sublimation took place, the mass of the ice was recorded as a function of time. With the sublimation complete, nitrogen was pumped into the chamber to return it to atmospheric pressure. Also shown in Figure 3 is the scattered spray due to nozzle end effects. This phenomenon will be discussed further in the proceeding section.

3.4 Results

Significant results were obtained for water exhausting into a vacuum. As water was injected into the chamber, it immediately froze due to the cooling which accompanies rapid expansion. The resulting stream of tiny ice particles impinged upon the impact plate forming a thin layer of ice. Accompanying this ice formation was a temporary pressure increase of approximately three orders of magnitude. This increase was due to the limited chamber volume and

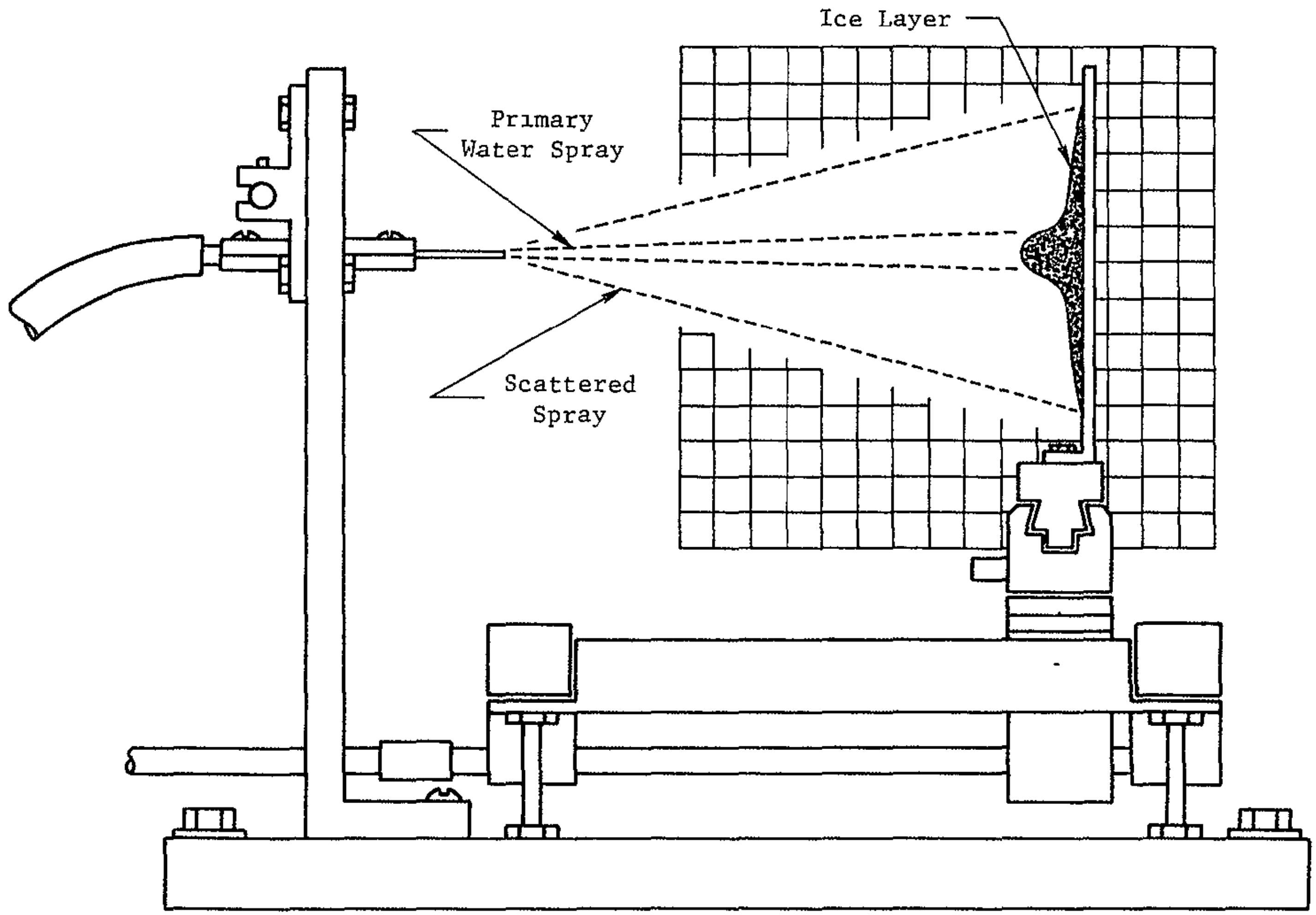

Figure 3. Experimental Ice Formation

pumping capacity, and was sufficient to cause a phase change in the accumulating ice. Initially, the accumulating ice was a rime ice, i.e., frosty and opaque. As the pressure increased this turned to a clear ice, i.e., smooth and translucent. After accumulation was complete the incoming water was shut off. Within 240 seconds the pressure had returned to its low value and the ice had reverted back to its rime phase. Photographs typical of water-ice accumulating and sublimating are presented in Figure 4. The pressure increase experienced in the laboratory facility should not adversly effect the operational application of the WST in space.

As the water was injected into the chamber it separated into two sprays: primary and scattered. It is believed that the scattered spray was due to nozzle end effects which may be eliminated through proper nozzle design. This spray resulted in a thin layer of ice forming on the impact plate. In contrast, the primary spray resulted in a thicker layer of ice being formed For an l/d of 269, the ratio of impact cross-sectional area to nozzle cross-sectional area was 530.

On the average, it took 2700 seconds for 0.002 kg of water-ice to sublime. However, several factors influenced the sublimation rate. The thinner the initial layer of ice the quicker it sublimed. This is seen in that the thin layer of ice due to the scattered spray sublimed faster than did the thicker layer from the primary spray. In addition, ice layers with larger surface areas also sublimed faster. The background pressure also effected the sublimation in that the higher the pressure the lower the sublimation rate. The effects of all these factors suggest that the sublimation rate is not a constant but varies with layer thickness, surface area, background pressure

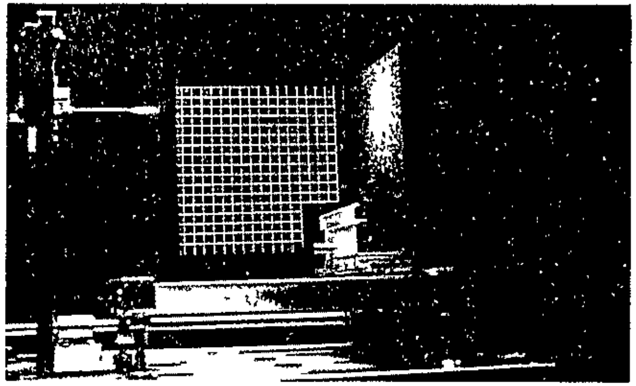

a. Water Spray Initiated at Time, t = -5.0 Seconds.

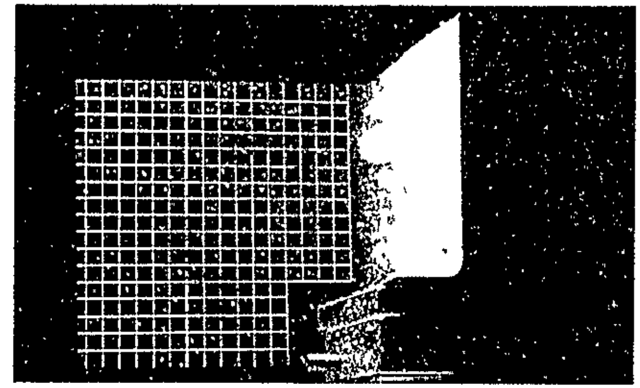

b. Accumulation Complete at Time, t = 0.0 Seconds.

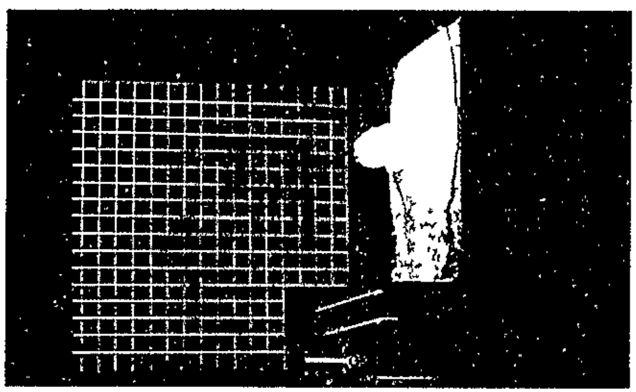

c. Sublimation Continuing at Time, t = 1800 Seconds.

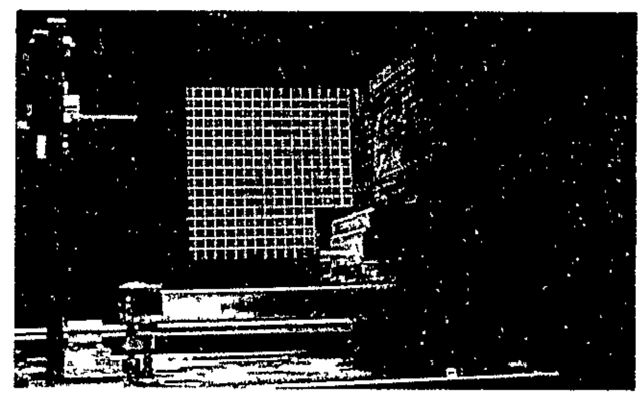

d. Sublimation Complete at Time, t = 2700 Seconds.

Figure 4. Photographs Typical of Water-Ice Accumulating and Sublimating.

and temperature.

Additional tests were conducted using 50% and 33% concentrations of ammonia hydroxide in water as the working fluid Problems were encountered with these tests, however, as the ammonia hydroxide reacted with the copper tubing which connected the reservoir to the nozzle. The resulting copper ammonia ion contaminated the solution, tinting it blue. Upon release into the chamber the solution froze with a translucent slushy appearance. Again, as the pressure was reduced a phase change occurred, changing the clear ice to rime ice. As sublimation took place, cubic millimeter size particles of ice seemed to explode from the surface of the main ice formation and cling to the insides of the vacuum chamber. This might be explained by the paramagnetism of the copper ammonia ion. Consequently, the sublimation rate was not observable.

Tests were also conducted using various concentrations of methanol in water, as illustrated in Figure 5. A 100% concentration of methanol was exhausted into the chamber, evaporating as fast as it was pumped in; no ice was formed. At a concentration of 50% the spray formed liquid drops on the impact plate which froze after 37 seconds. Similar results were obtained using a 33% concentration. At this concentration liquid drops formed which took 120 seconds to freeze In both cases it took approximately 900 seconds for the small drops to sublime. At 20% and 10% concentrations, the spray formed a slush upon contact with the impact plate. After 1500 seconds the slush had solidified, turning into an opaque rime ice. At a concentration of 10% it took 1050 seconds for 0.002 kg of ice to sublime.

Although only qualitative in nature, these results compare

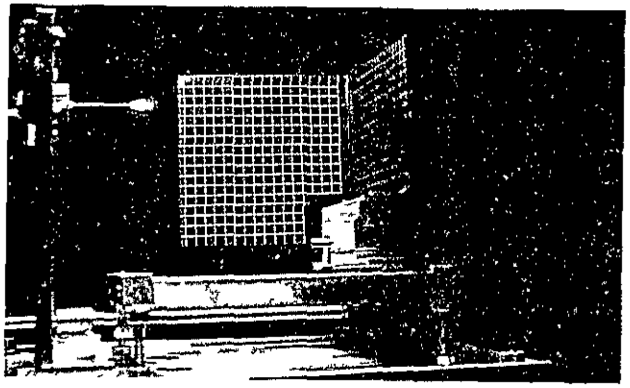

a. Complete Evaporation, No Ice Formation at 100% Concentration.

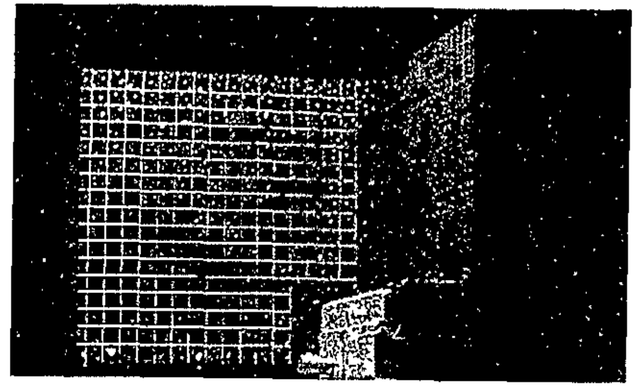

b. Liquid Drop Formation at 50% Concentration.

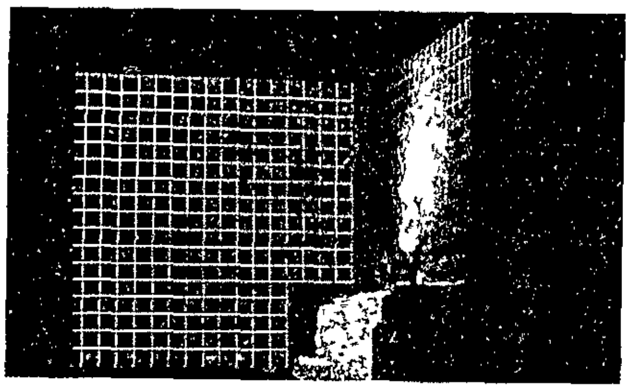

c. Slush Formation at 20% Concentration, Time, t = 30 Seconds.

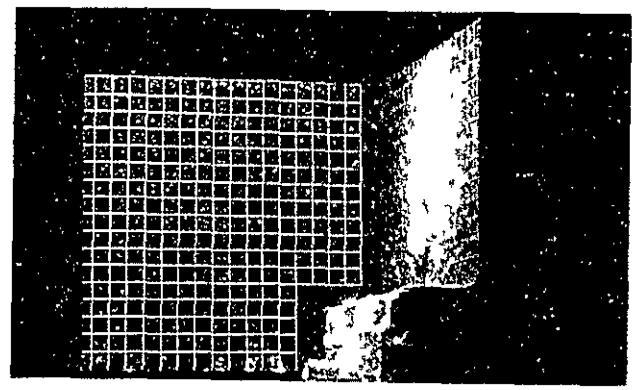

d. Solidified Rime Ice at 20% Concentration, Time, t = 1500 Seconds.

Figure 5. Photographs Typical of Various Concentrations of Methanol in Water Accumulating and Sublimating.

favorably with previous investigations. The sublimation rate determined for water is supportive of the 1100 second exponential folding time observed by Sharma (7). The effect of additives, such as ammonia and alcohol, is to increase the sublimation rate as observed by Watson (6).

CHAPTER IV

ANALYSES

The analyses of the WST were divided into two parts. First to be considered were the equations of motion for a vehicle being despun or detumbled via the WST. Secondly, these equations of motion were programmed on a digital computer to simulate the despin operation. Results of the analyses are presented and include water mass requirements, despin times and despin profiles.

4.1 Equations of Motion

The equations of motion for a spacecraft being detumbled or despun by means of the WST, were derived using both a control volume analysis and an angular momentum balance. A rigorous derivation of the equations of motion following the control volume analysis of Grubin (8), resulted in a set of first order nonlinear differential equations coupled in $\vec{\omega}$. These equations were most general and applied to any arbitrary vehicle with arbitrary components of angular velocity. However, included in the resulting equations were integrations over the tumbling vehicle's surface which, except in the case of simple geometries, would have been difficult to solve and provided very little insight into the problem. For these reasons, the control volume approach was excluded from further consideration.

In order to provide more physical insight into the problem, an angular momentum balance was performed (9). The water spray was assumed to possess low momentum, imparting negligible torque to the spinning vehicle. Furthermore, it was assumed that sublimation occurred radially such that the net torque was negligible. An additional simplification was to assume that a spacecraft's complex geometry may be represented by an equivalent cylindrical body. The equivalent cylindrical body has the same moment of inertia about the spin axis and same surface area as the original spacecraft. Figure 6 illustrates the angular momentum balance model in which a low momentum water spray impinges upon the circumference of a cylinder spinning about its axis of symmetery. A thin ice layer forms over its surface which sublimes, carrying away momentum with it. The momentum balance between the vehicle's angular momentum h_v and the ice's momentum h_w can be written in differential form as

$$-dh_v = dh_w \tag{1}$$

The vehicle's angular momentum is expressed as

$$h_v = I\ \omega \tag{2}$$

where I is the vehicle's moment of inertia about the axis of rotation and ω is its corresponding angular velocity. Assuming I to be constant and differentiating

$$dh_v = I\ d\omega \tag{3}$$

For the water making up the thin ice layer illustrated in Figure 6, its angular momentum may be expressed in differential form as

$$dh_w = r^2\ \omega\ dm \tag{4}$$

with r being the perpendicular distance from the axis of rotation to the ice with mass m. Substitution of equations (3) and (4) into (1)

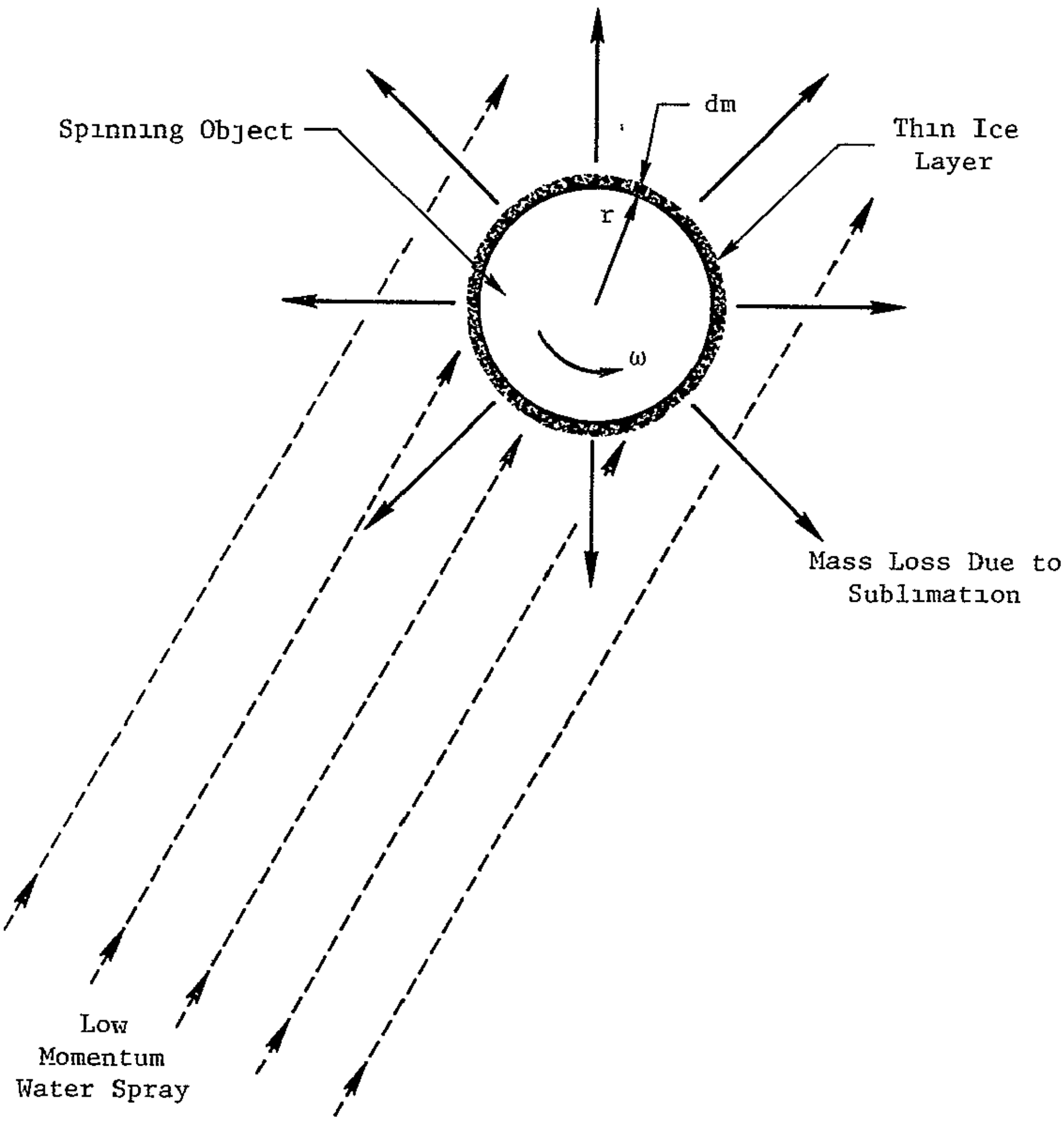

Figure 6. Angular Momentum Balance Model

yields the differential form of the angular momentum balance

$$-I\ d\omega = r^2\ \omega\ dm \tag{5}$$

Integrating

$$-I\ \text{Ln}\ \omega\Big|_{\omega_i}^{\omega_f} = r^2\ m \tag{6}$$

where ω_i and ω_f are the initial and final spin rates respectively. Solving for m

$$-\frac{I}{r^2}\ \text{Ln}\ \frac{\omega_f}{\omega_i} = m \tag{7}$$

This equation expresses the mass of water required to stick to the vehicle as a function of its initial and final spin rates. Note that the minus sign insures that ω_f will always be less than ω_i. Only a fraction of the water being sprayed from the retrieval craft actually sticks to the spinning vehicle. Thus, the total water mass sprayed m_t may be expressed as

$$m = k\ m_t \tag{8}$$

where k is a coefficient of accumulation, i.e., the ratio of total water mass sprayed to that which sticks to the target, with values

$$0 \leq k \leq 1 \tag{9}$$

Obviously the crew of the shuttle must wait until the ice sublimes in order to actually capture the object. Using an average value for the sublimation rate ν, the time t for the ice with surface area a to sublime is

$$t = \frac{m}{\nu\ a} \tag{10}$$

4.2 Computer Simulation

A computer program was written to simulate the WST in operation. The program consisted of modeling the angular momentum balance developed in the previous section on an IBM 370/168 digital computer. It has been assumed that each satellite had an initial spin rate of 30 rpm and its inertia can be estimated from its mass. It was also assumed that the flow rate of water to the object was equal to the sublimation rate. The final spin rate was choosen to be 0.6 rpm, a 98% reduction in angular momentum. The program calculated total water mass requirements and despin times as a function of satellite mass and coefficient of accumulation Typical despin profiles for a 200 kg satellite were also calculated. The complete results are presented in the following section.

4.3 Results

Satellite despin performance parameters have resulted from the computer simulated water spray retrieval operation. Of primary interest were the total water mass requirements for a complete despin. Figure 7 is a graph of total water mass requirements as a function of satellite mass and coefficient of accumulation. Assuming a realistic value for k to be between 0.05 and 0.5, for a spacecraft up to about 800 kg the amount of water required to despin it is well within the shuttle payload capabilities outlined in Appendix A. These water mass requirements are of the same order of magnitude as those estimated for the water jet technique (2).

An additional consideration is the time required to despin an object. Obviously the crew of the shuttle must wait until the water

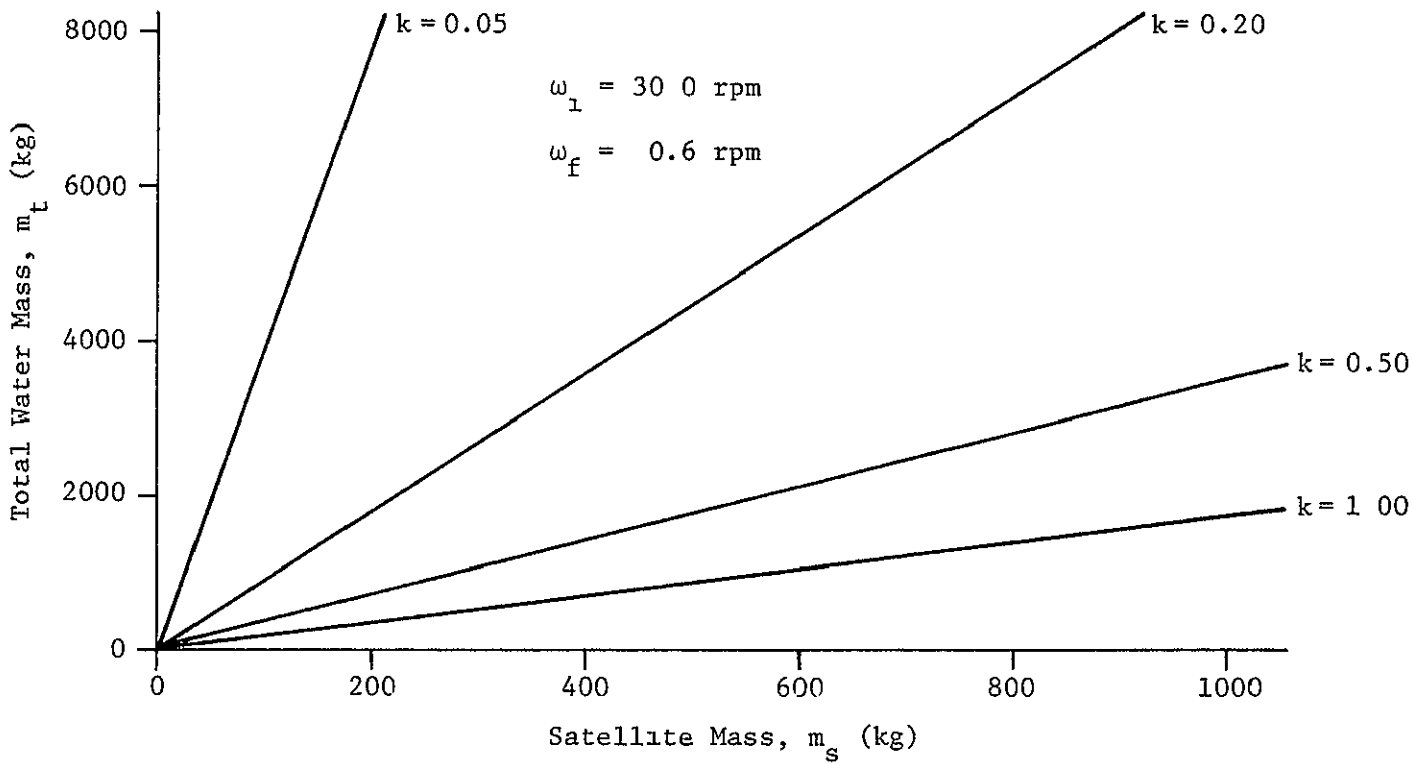

Figure 7 Total Water Mass Requirements for a 98% Reduction in Angular Momentum.

sublimes in order to actually capture an object. This is why the sublimation rates are critical with regard to this technique. Figure 8 summarizes the results of calculations of despin times Sublimation rates used are discussed in the preceeding chapter. Assuming a coef-ficent of accumulation between 0.05 and 0.5, the despin time required for satellites up to 800 kg mass ranges from a few minutes to about two hours.

Figure 9 shows some typical despin profiles for different coefficients of accumulation. In all cases the despin profile is expon-ential. This particular figure is for a satellite of 200 kg mass.

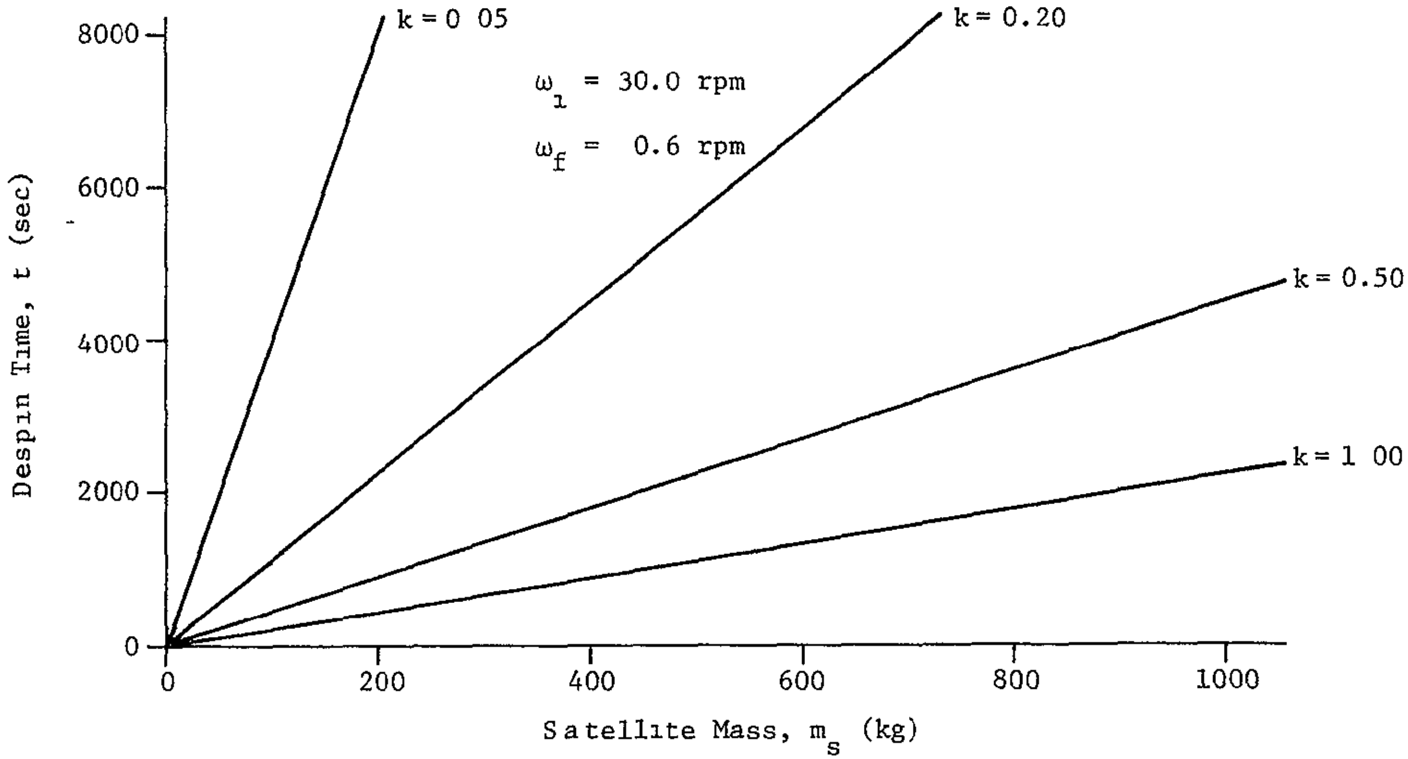

Figure 8 Despin Times for a 98% Reduction in Angular Momentum.

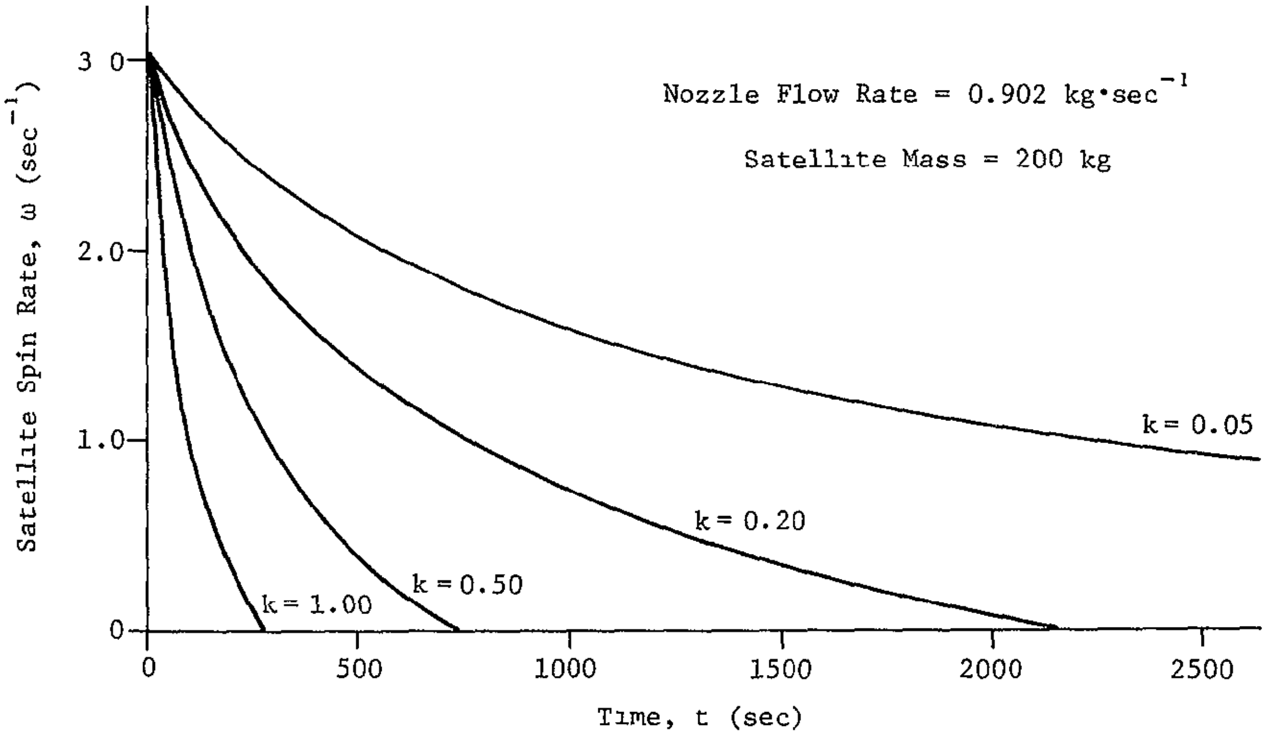

Figure 9 Typical Satellite Despin Profiles.

CHAPTER V

EXAMPLE APPLICATION: OSO - 5 RETRIEVAL

As an example of a potential application of the WST, the retrieval of a disabled satellite was considered. Included in this example application were four areas of investigation: satellite selection, passivation, capture and stowage. For the satellite selected, despin times and total water mass requirements were computed. Conceptual designs of the spray, capture and stowage mechanism have also been included.

5.1 Satellite Selection

Prior to the selection of a satellite to be despun and retrieved, a selection criteria was established. The particular satellite selected had to be:

1. A U.S. satellite, preferably of NASA origin.
2. Compatible with size and mass limitations for shuttle payload.
3. Its orbit must be reachable by the shuttle.

Applying these criteria to a survey of satellites presently in orbit, a selection was made.

The shuttle retrieval envelope is illustrated in Figure 10. This figure depicts a summary of shuttle orbit capabilities with respect to semimajor axis, inclination and deliverable payload. It also illustrates the effect of launch site and the use of orbital maneuvering subsystem (OMS) kits on the attainable orbits. Additional

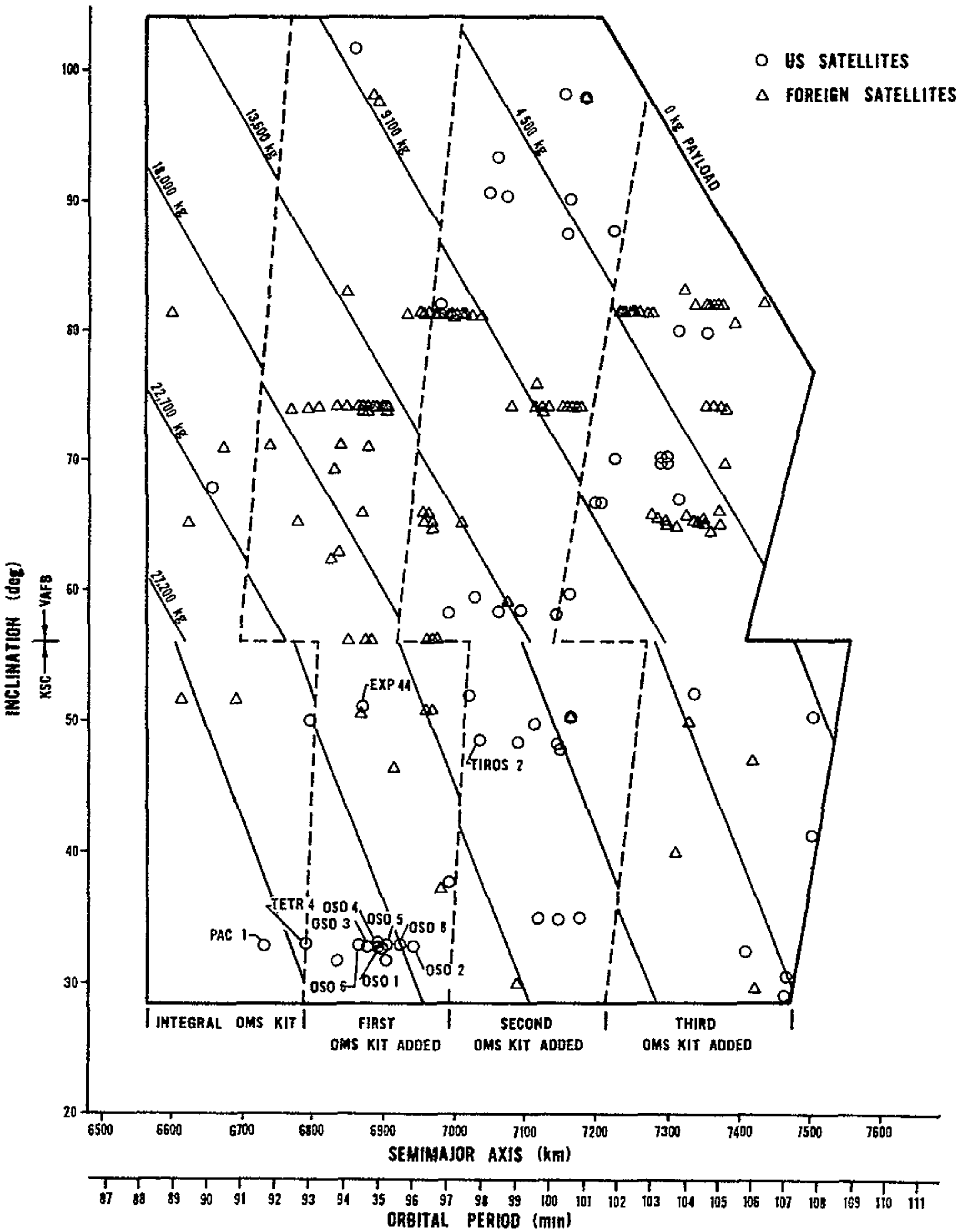

Figure 10. Shuttle Retrieval Envelope (10)(11).

shuttle orbit and payload capabilities are presented in Appendix A. In addition to shuttle capabilities, Figure 10 shows a complete set of satellites which are reachable by the shuttle. These consist of spacecraft launched up to June 30, 1976 and include U.S. and foreign spacecraft. For a detailed listing of each individual satellite and its orbital parameters, refer to Appendix B.

A final list of candidate satellites was obtained by eliminating those satellites within the shuttle retrieval envelope which are too large or massive to be retrieved. In addition, only those satellites with inclination between 32.0 and 57.0 degrees, i.e., within the proposed inclination range for the first six shuttle orbital flight tests (12), were considered. Table IV lists the resulting candidate satellites; Figure 10 shows their positions. Of these, OSO - 5 Orbiting Solar Observatory, was selected on the rationale that it presents a fairly severe combination of the individual conditions which make retrieval difficult· weight, size and spin rate There are heavier, larger, or faster spinning candidate satellites, but an example based on OSO - 5 will be illustrative of the problems associated with the middle range of each of these conditions.

The OSO - 5 is the fifth in a series of eight scientific satellites designed as a vehicle for experiments which collect solar and celestial navigation data. It was manufactured by Ball Brothers Research Corporation, Boulder, Colorado for NASA's Goddard Space Flight Center and launched on 22 January 1969 from Kennedy Space Center. It contains eight primary scientific instruments furnished by U.S. government agencies, and U.S., British and French universities it was successfully operated until 1974, when it was placed in a safe,

Table IV

Candidate Satellites for Despin and Retrieval

Name		Launch Date	Semimajor Axis (km)	Inclination (deg)	Mass (kg)	Diameter (m)	Width (m)	Initial Spin Rate (rpm)
Tiros	2	Nov 60	7038	48.5	126	--[a]	--[a]	10
OSO	1	Mar 62	6901	32.8	208	2.34	0.94	30
OSO	2	Feb 65	6939	32.8	247	2.34	0.94	30
OSO	3	Mar 67	6890	32.8	284	2.57	0.79	30
OSO	4	Oct 67	6897	32.9	271	2.57	0 94	30
OSO	5	Jan 69	6908	32.9	291	2.34	0.97	30-40
OSO	6	Aug 69	6865	32.9	290	2.34	0.94	30-40
PAC	1	Aug 69	6736	32.9	120	1.35	4 88	--[a]
EXPLORER	44	Jul 71	6879	51.0	118	0.76	0.58	60
TETR	4	Sep 71	6795	33.0	20	0.30	0.30	--[a]
OSO	8	Jun 75	6924	32.9	1066	3.07	2.11	6

[a] Data not available.

stowed mode of operation.

The OSO-5 has a diameter of 1.12 m and height of 0.97 m, as shown in Figure 11. In the launch condition, the arms were folded alongside the third stage of the launch vehicle. Total launch weight was 291 kg. Additional mass and inertia properties are given in Table V.

The spacecraft consisted of two main structural sections: the rotating wheel, and the solar-oriented sail The wheel consists of nine wedge-shaped compartments arranged around the central hub and azimuth shaft assembly. Four of the compartments housed the wheel control electronics Attached to three compartments are the extendible arms supporting the spin control gas bottles and reaction jets. These arms are released from the stowed state during the launch sequence and moved upward into the plane of the wheel, thereby increasing its effective diameter and spin moment of inertia. The wheel and sail are connected by the azimuth shaft assembly, which includes appropriate bearings and azimuth shaft, and allows the pointed instruments to be pointed toward the sun.

When operational, the sail structure maintained a fixed inertial attitude and the wheel structure rotated at between 27 and 39.6 rpm. In its nonoperating mode, however, both parts rapidly equalize their rates due to bearing friction. Calculations show that the current angular rate is approximately 25 rpm.

5.2 Satellite Passivation

The elimination of OSO-5 angular momentum was considered as an example application of the WST. Figure 12 illustrates the

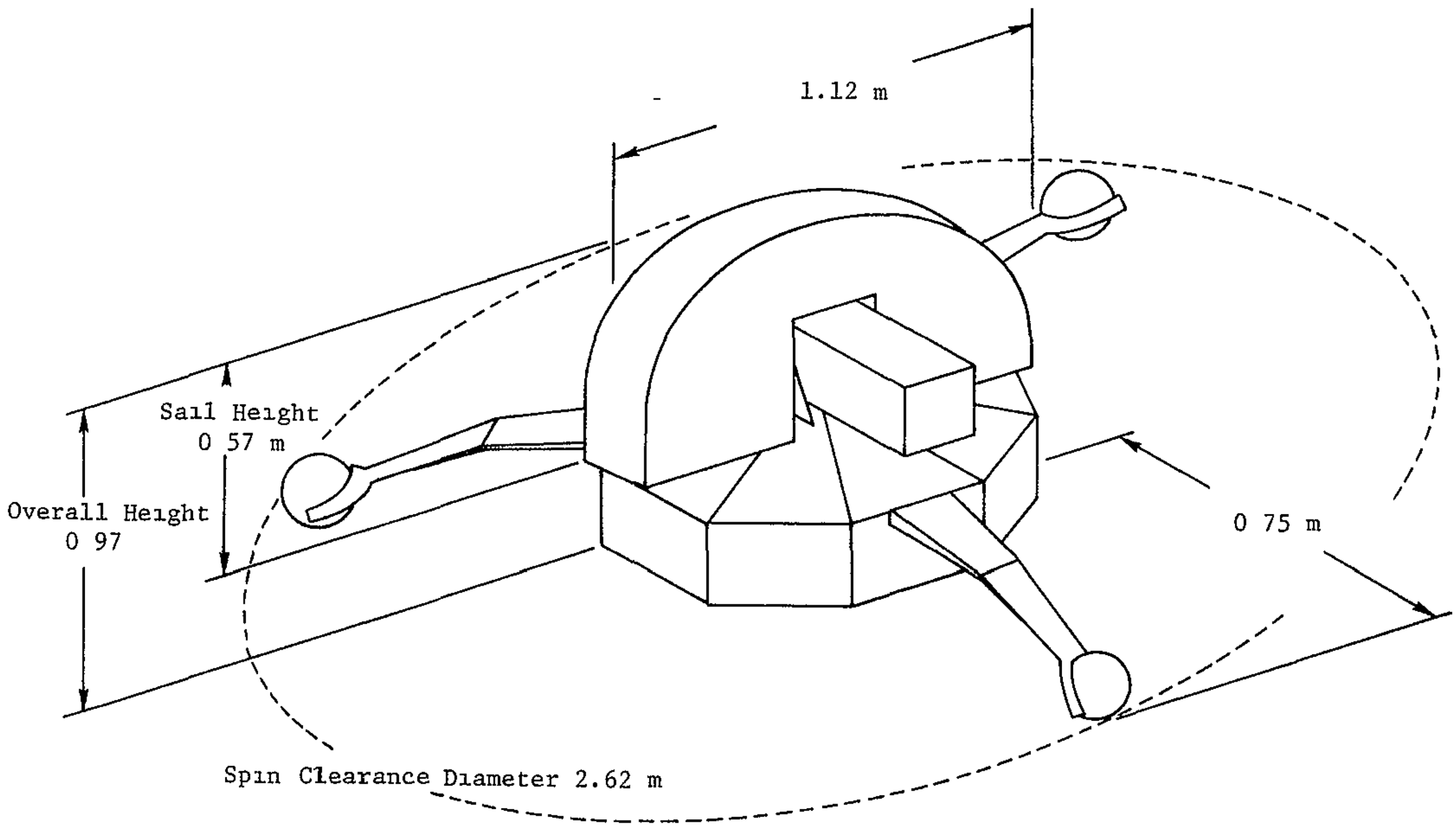

Figure 11. OSO - 5 Overall Dimensions (13)

Table V

OSO - 5 Mass and Inertia Properties

Properties	Measured or Calculated Values	
Launch Mass (kg)	291	
Spin Moment of Inertia - Wheel ($N \cdot m \cdot s^2$)	18.70	Arms Down
	24.61	Arms Up
Spin Moment of Inertia - Wheel and Sail ($N \cdot m \cdot s^2$)	21.67	Arms Down
	27.59	Arms Up
Average Transverse Moment of Inertia ($N \cdot m \cdot s^2$)	17.70	Arms Down
	18.13	Arms Up
Ratio of Spin MOI to Transverse MOI	1.36	Arms Up

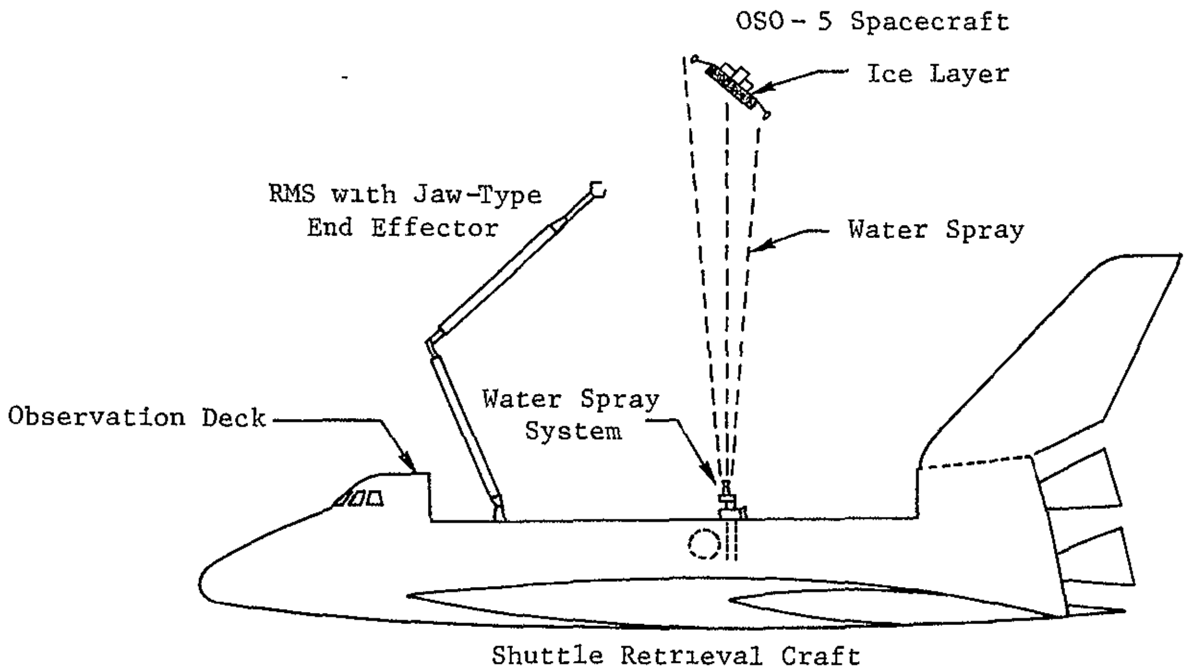

Figure 12. OSO - 5 Retrieval Operation

scheme used for this operation. Water is sprayed from the shuttle retrieval craft, impinging upon OSO-5, quickly freezing, forming a thin layer of ice over portions of its surface. In this design the nozzle, water and associated hardware are located in the shuttle payload bay. One possible spray system is shown in Figure 13, mounted on an orbital flight test pallet. This system consists of two spherical water storage tanks with 500 kg capacity each. The tanks are lined with flexible rubber bladders. When pressurized by the small nitrogen tank, water is forced to the nozzle where it is then sprayed. The nozzle is pointed via controlled inputs from the shuttle observation deck, making an extravehicular activity (EVA) unnecessary. Low power heaters may be incorporated into the nozzle design to prevent freezing and eventual blocking of the nozzle.

The equations of motion developed previously were used to simulate the despin of OSO-5 via the WST. Using the mass and inertia properties listed in Table V, and assuming an initial spin rate of 25 rpm, total water mass requirements and despin times were calculated. The results of these calculations are graphed in Figures 14 and 15 for various values of k. For a k value of 0.50, the total water mass necessary to eliminate 98% of the angular momentum is less than 700 kg The associated despin time is on the order of 700 seconds.

5.3 Satellite Capture

Having despun OSO-5, the capture sequence begins. As illustrated in Figure 12, the actual capture of OSO-5 is performed using the remote manipulator system (RMS) with a jaw-type end effector. Recieving controlled inputs from the shuttle observation deck, the RMS

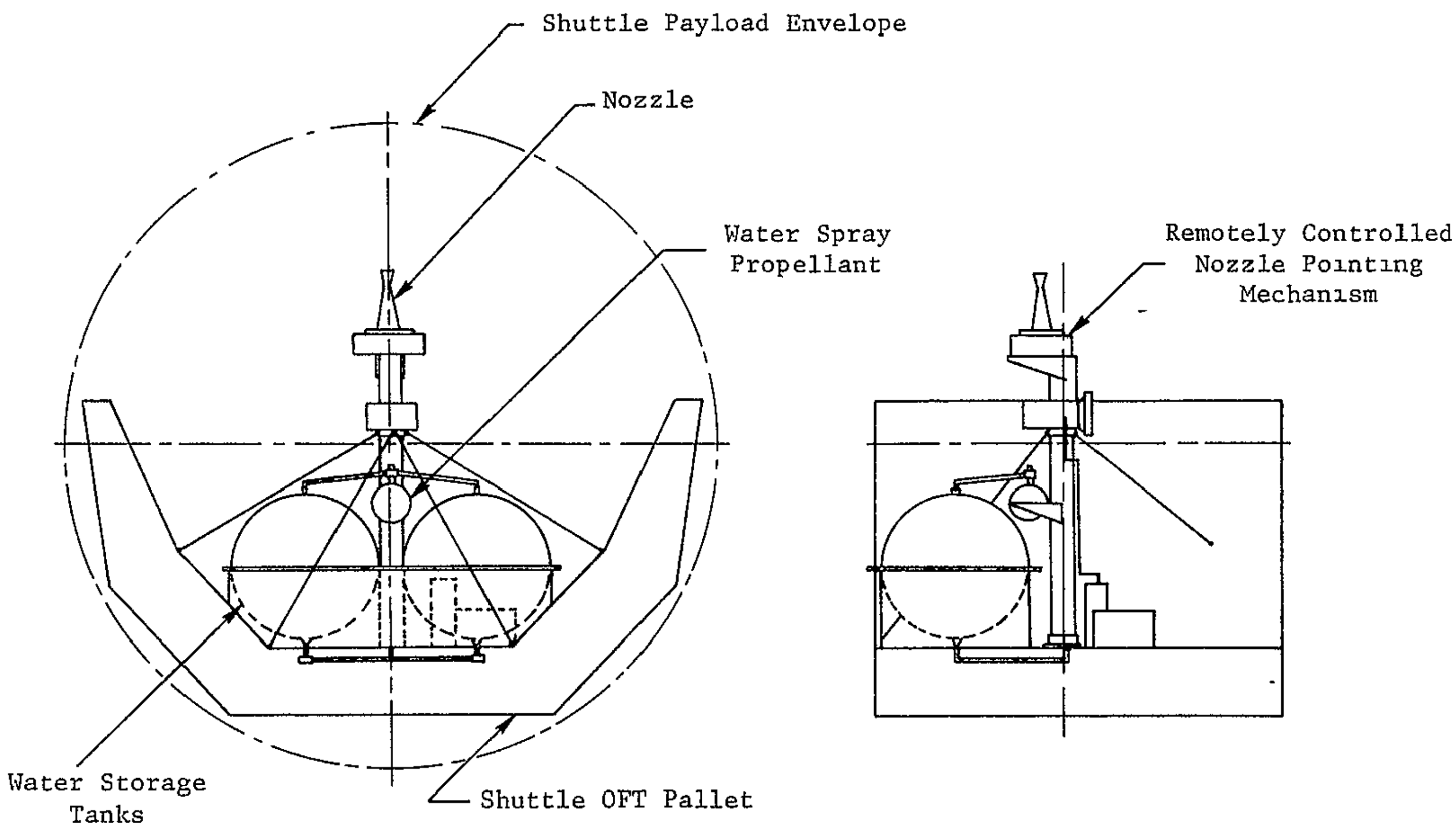

Figure 13 Pallet Mounted Water Spray System.

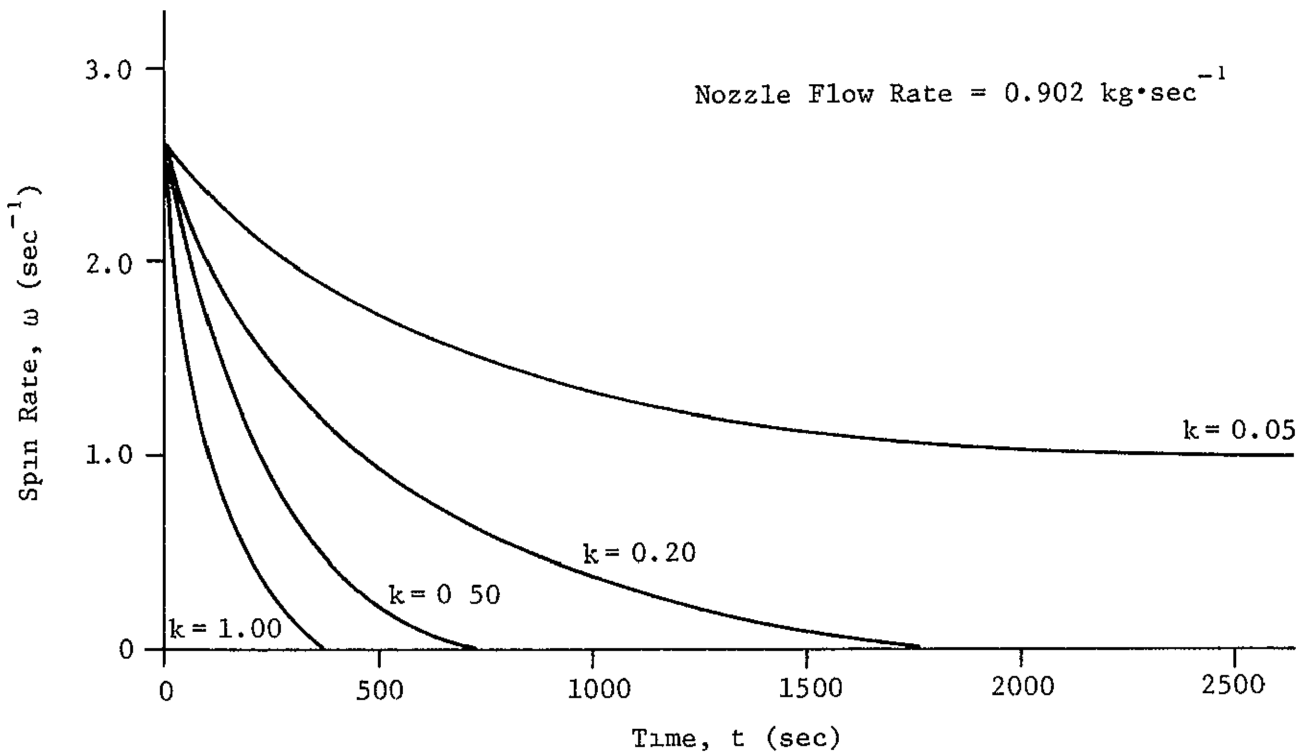

Figure 14. Typical Despin Profiles for the OSO - 5 Spacecraft

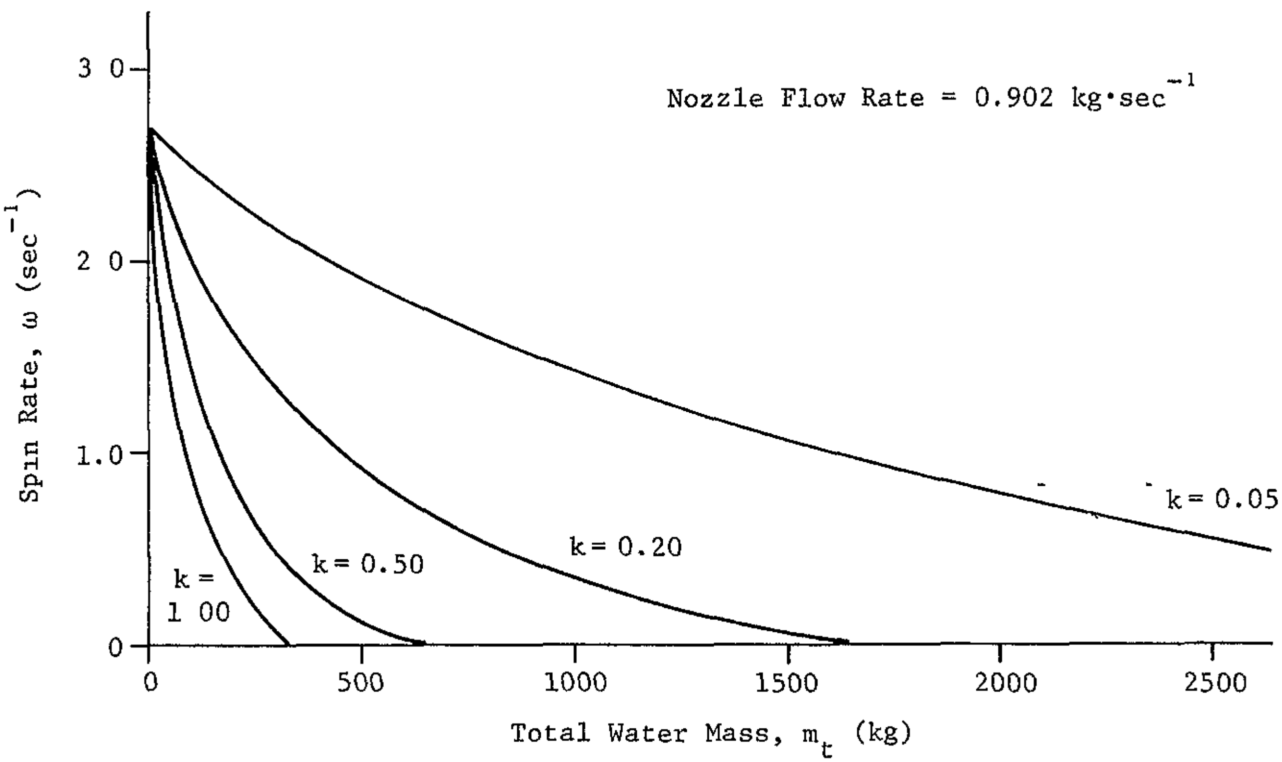

Figure 15 Total Water Mass Requirements for Despinning the OSO-5 Spacecraft

moves the mechanical jaws into position about one of the OSO - 5 arms. The jaws close, capturing the spacecraft in its grip. The RMS then returns to the shuttle bay with the satellite for stowage and return.

5.4 Satellite Stowage

The stowage of OSO - 5 in the shuttle bay is illustrated in Figure 16. This scheme employs a specially designed hydraulic grappler which holds the spacecraft securely in place through reentry and landing. The conceptual design of this grappling mechanism is illustrated in Figure 17. In use, the RMS positions OSO - 5 such that its attachment fitting, i.e., the mount which originally attached the spacecraft to the launch vehicle, is positioned within the hooks of the hydraulic grappler. Once in place, a signal is automatically fed back to the control logic which pressurizes the grappler mechanism causing it to contract, locking tightly around the attachment fitting. This stowage operation is controlled from the shuttle observation deck, making an EVA unnecessary.

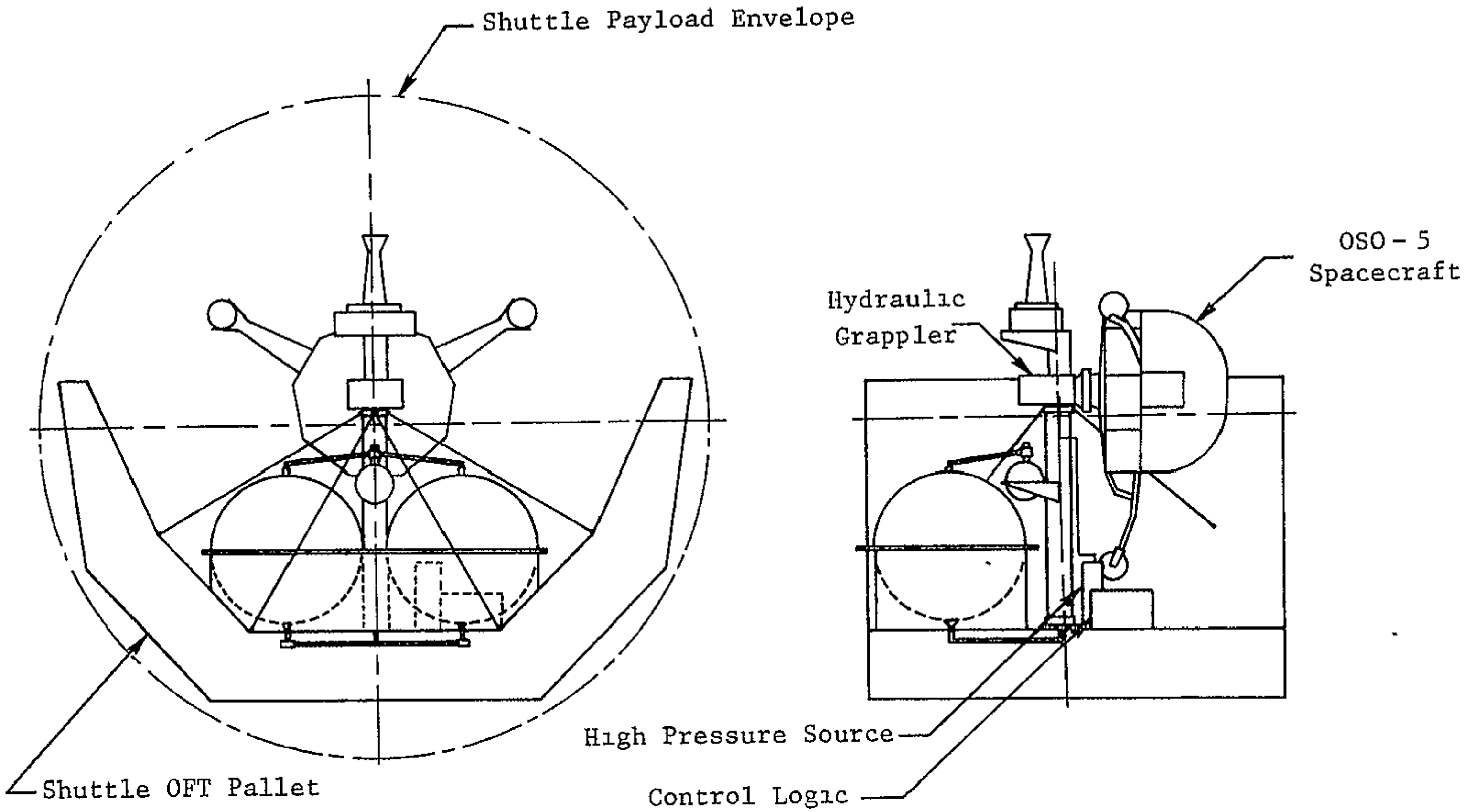

Figure 16 OSO - 5 Stowage for Reentry and Landing

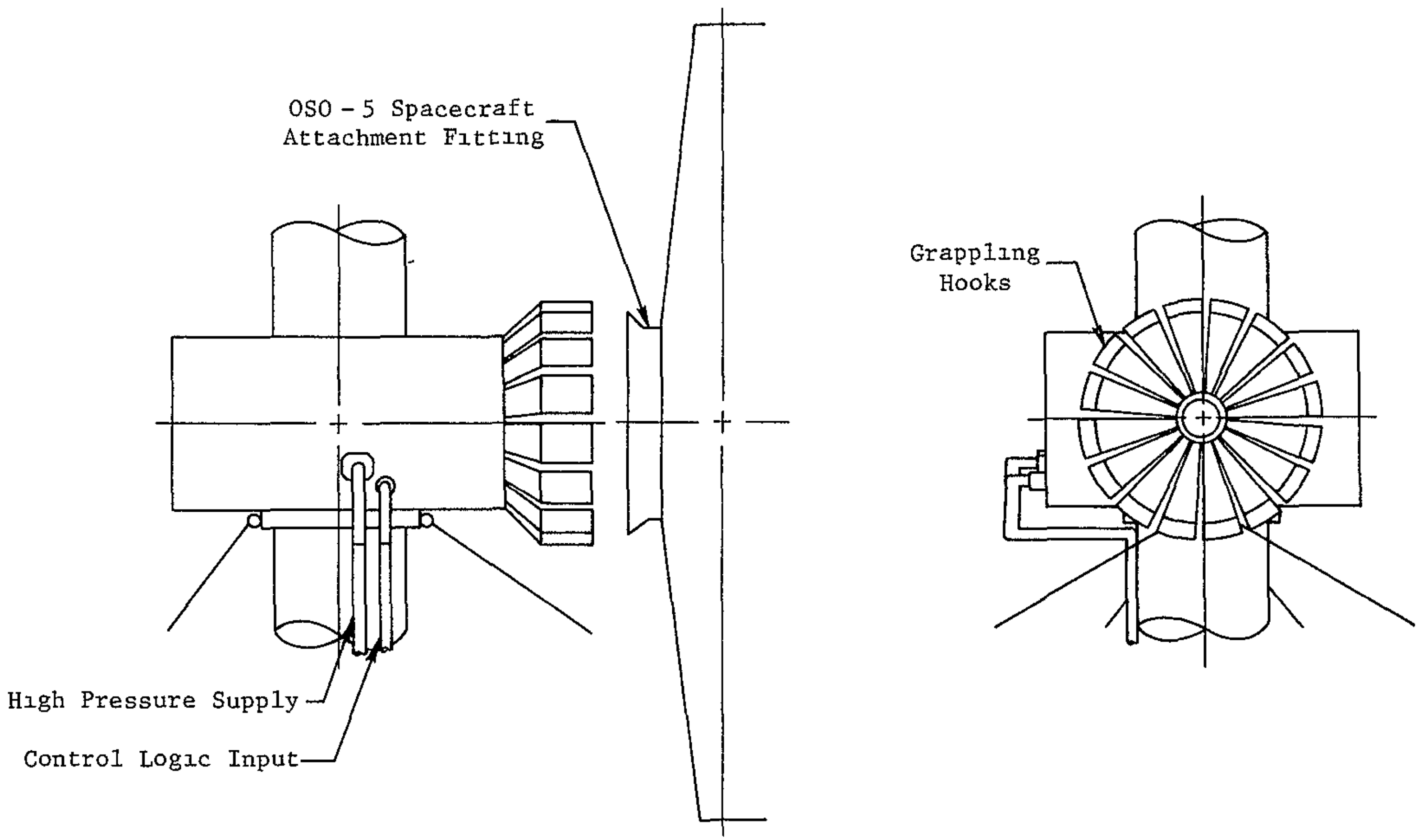

Figure 17 Hydraulic Grappling Mechanism.

CHAPTER VI

CONCLUSIONS

A new and safe technique for eliminating angular momentum of disabled spacecraft has been presented here. This would appear to be an ideal method of despinning because the required logic is extremely simple and there are no safety hazards involved. Furthermore, the working part of the system has essentially no cost and is expendable and need not be brought back to earth.

Experimental results have indicated that the accumulation and sublimation of ices in a space-like environment is compatible with the total concept of the water spray retrieval operation. The results show that water freezes almost immediately upon exhausting into a vacuum, and sublimes slower than other ices tested. The effects of additives like alcohol is to increase the sublimation rate which results in a faster retrieval operation. In addition, the proper concentration of alcohol in water can delay freezing of the mixture until it contacts the spinning vehicle. Several factors were seen as effecting the sublimation rate: ice layer thickness, surface area, background pressure and temperature. The results also show that proper nozzle design must be considered to keep dispersion at a minimum

Based on the assumptions and calculations made in this investigation, it would appear that most old spacecraft in orbits reachable by the space shuttles can be retrieved if spinning, through the use of the WST. During the operational application of this technique, it may be required for the crew to wait up to two hours in order to actually capture the object. This is not seen as a major deterrent in its application. Furthermore, the associated masses of water which must be carried into orbit are relatively low compared to the maximum capability of the space shuttle.

Further testing and analyses are required before operational use and investments are made for development. These tests should include actual orbital flights which are now under consideration.

REFERENCES

1. Canetti, G.S., "Safety in Earth Orbit Study," Final Report, Rockwell International, SD 72-SA-0094, Vol. III, NASA Contract NAS9-12004, July 1972.

2. Canetti, G.S., "Recovery From a Tumbling Condition in Space," IAF Paper No. A-76-04, Presented at the 27th Congress of the I.A.F., Anaheim, October 10-16, 1976.

3. Kaplan, M.H., "Despinning and Detumbling Satellites in Rescue Operations," Proceedings of the Fifth International Space Rescue Symposium, International Academy of Astronautics, May 1973, pp. 225-243.

4. Kaplan, M.H., "Technical Problems Related to Orbital Capture of Passive Objects," Third Semi-Annual Progress Report Under NASA Grant NSG-7078, The Pennsylvania State University, 1975.

5. Kaplan, M.H. and Freesland, D.C., "Use of Water Sprays in Space Rescue and Retrieval Operations," IAF Paper No. A-76-09, presented at the 27th Congress of the I.A.F., Anaheim, October 10-16, 1976.

6. Watson, Murray and Brown, "The Stability of Volatiles in the Solar System," Icarus 1, pp. 317-327.

7. Sharma, R.D. and Buffalano, C., "Temperature and Size Histories of Liquid H_2, O_2, and H_2O Particles Released in Space," Journal of Geophysical Research, Vol. 76, No. 1, January 1971, pp. 232-237.

8. Grubin, C., "Mechanics of Variable Mass Systems," Franklin Institute Journal, Vol. 276, October 1963, pp. 305-312.

9. Kaplan, M.H., Modern Spacecraft Dynamics and Control, John Wiley and Sons, New York, 1976, Chapter 2.

10. "Space Shuttle Systems Payload Accomodations," NASA Johnson Space Center, JSC-07700, Vol. XIV, December 1976, Chapter 3

11. "Satellite Situation Report," NASA Goddard Space Flight Center, Vol. 16, No. 3, June 1976.

12. "Announcement of Opportunity for Space Shuttle Orbital Flight Test Program," NASA A.O. No. OPPI-76-1, September 1976, p. 4.

13. "OSO-5 Orbiting Solar Observatory," Final Report Prepared Under NASA Contract NAS5-9300, Ball Brothers Research Corporation, April 1971.

APPENDIX A

SPACE SHUTTLE PAYLOAD CAPABILITY

The space shuttle payload delivery capabilities are outlined in the following figures. Figures 18 and 19 graph payload mass as a function of circular orbital altitude for Kennedy Space Center (KSC) and Vandenberg Air Force Base (VAFB) launches respectively. The addition of orbital maneuvering subsystems (OMS) kits is also shown. Figure 20 graphs payload mass versus orbit inclination. Again, the effects of additional OMS kits are included. For the purpose of constructing these figures, both delivery and rendezvous maneuvers have been included in computing payload masses.

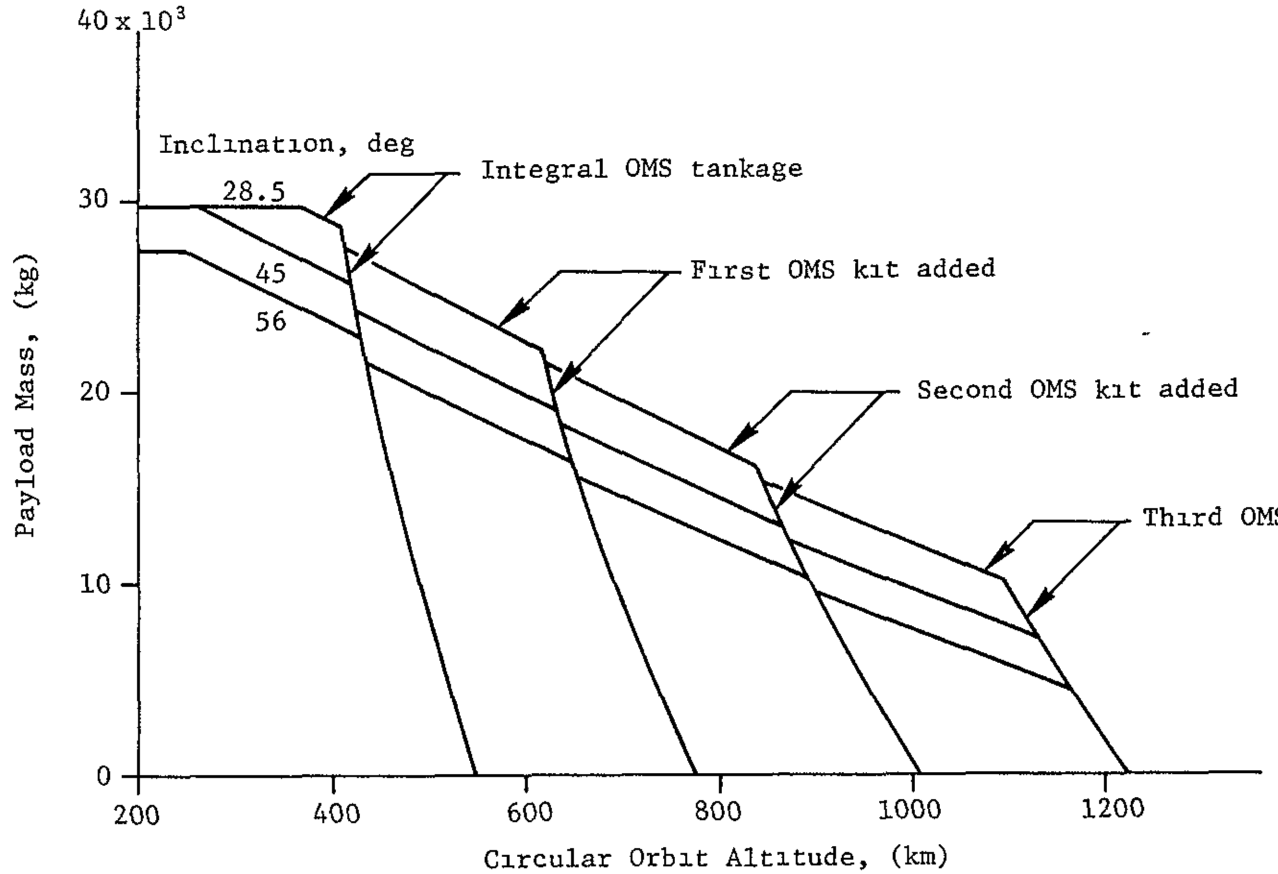

Figure 18 Payload Mass Versus Circular Orbital Altitude - KSC Launch, Delivery and Rendezvous (10)

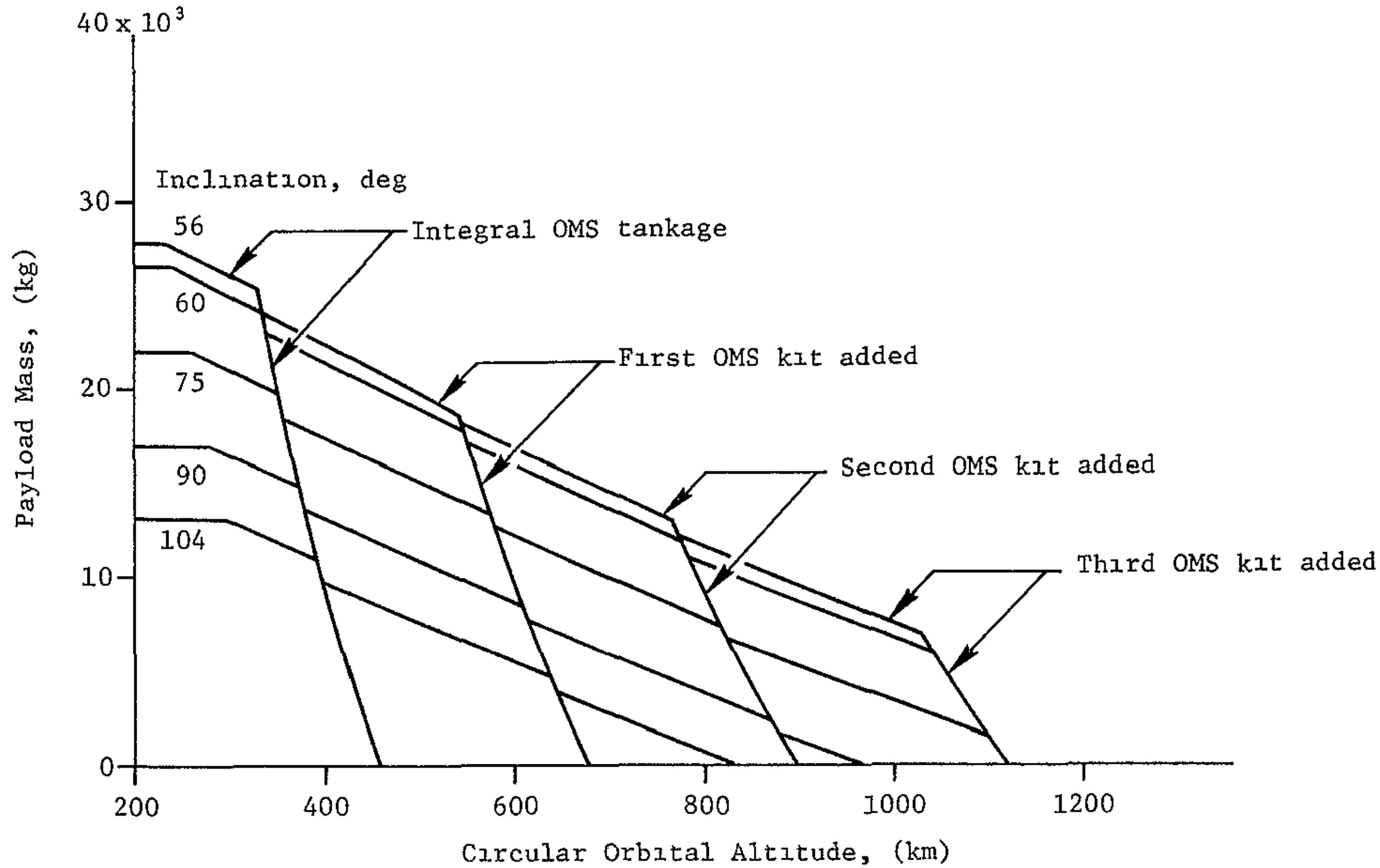

Figure 19 Payload Mass Versus Circular Orbital Altitude - VAFB Launch, Delivery and Rendezvous (10).

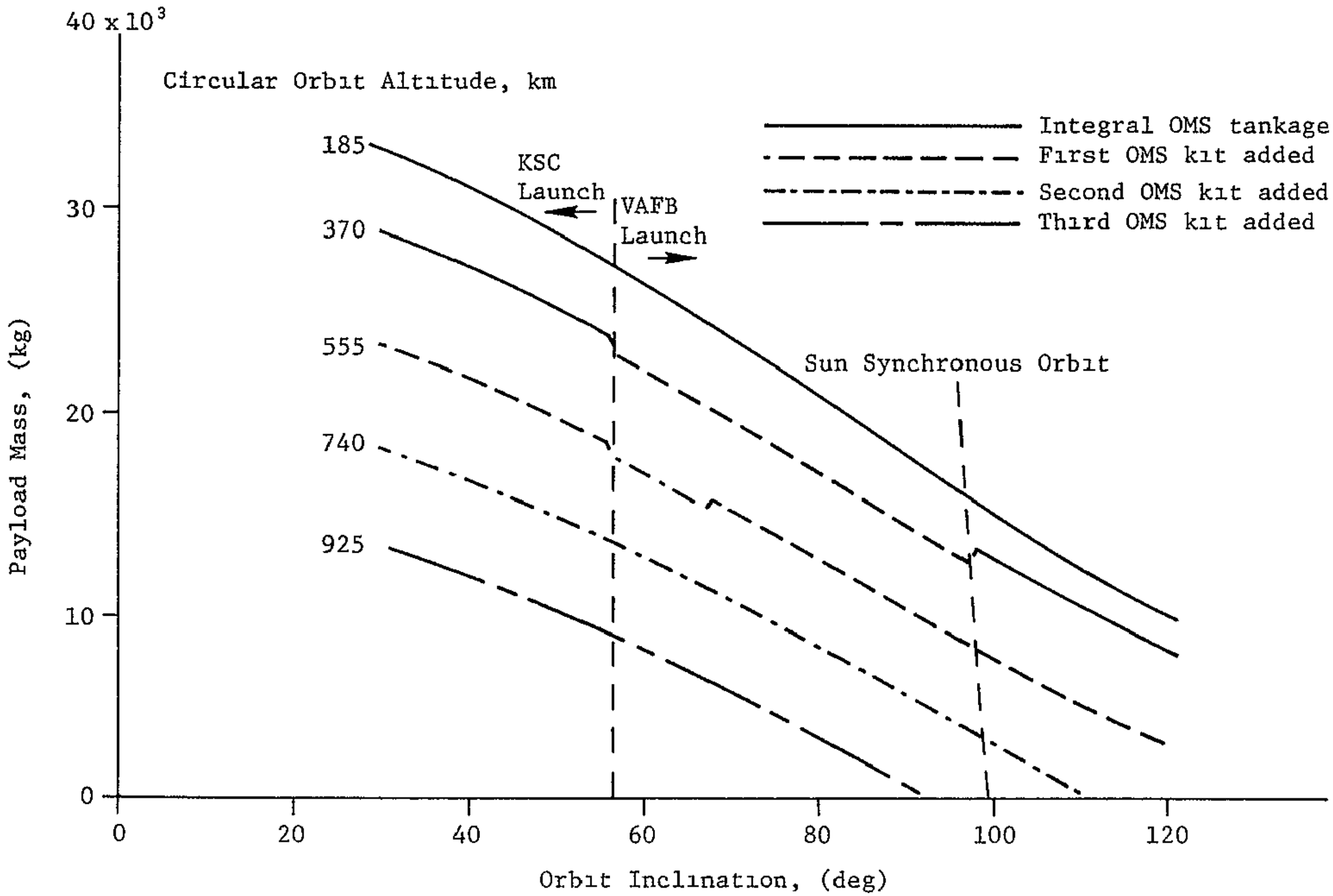

Figure 20. Payload Mass Versus Inclination for Various Circular Orbital Altitude, Delivery and Rendezvous (10).

APPENDIX B

SATELLITES WITHIN THE SHUTTLE RETRIEVAL ENVELOPE

Orbital data is tabulated for those satellites within the shuttle retrieval envelope given in Figure 10. Table VI includes U.S. satellites while Table VII includes foreign satellites Satellite name, international designation, period and inclination are listed. These tables have been constructed from data compiled by NASA (11).

Table VI

U.S. Satellites Within the Shuttle Retrieval Envelope (11)

Name	International Designation	Period (min)	Inclination (deg)
Explorer 7	1959 IOTA 1	100.6	50.3
Tiros 1	1960 BETA 2	99.0	48.3
Transit 2A	1960 ETA 1	101.4	66.6
GREB	1960 ETA 2	101.3	66.6
Tiros 2	1960 PI 1	97.9	48.5
Explorer 11	1961 NU 1	107.1	28.8
Transit 4A	1961 OMICRON 1	103.7	66.8
INJUN SR3	1961 OMICRON 2	103.7	66.8
Tiros 3	1961 RHO 1	100.3	47.8
Transit 4B	1961 A ETA 1	105.7	32.4
TRAAC	1961 A ETA 2	105.7	32.4
Tiros 4	1962 BETA 1	100.2	48.2
OSO 1	1962 ZETA 1	95.1	32 8
Tiros 5	1962 A ALPHA 1	100.2	58.0
Tiros 6	1962 A PSI 1	98.5	58.3
ANNA 1B	1962 B MU 1	107.8	50.1
Explorer 16	1962 B CHI 1	104.3	52.0
Transit 5A	1962 B PSI 1	98.3	90.6
Tiros 7	63024 A	97.0	58.2
Research Satellite for Geophysics	63026 A	99.5	49.7
Centaur 2	63047 A	107.0	30.3
Tiros 8	63054 A	99.2	58 4

Table VI (continued)

U.S. Satellites Within the Shuttle Retrieval Envelope (11)

Name	International Designation	Period (min)	Inclination (deg)
Gravity Gradient 1	64001 B	103.3	69.9
EGRS	64001 C	103.4	69.8
Solarad	64001 D	103.4	69.9
Explorer 20	64051 A	103.8	79.8
Explorer 22	64064 A	104.6	79.6
Explorer 23	64074 A	97.6	51.9
OSO 2	65007 A	95.9	32.8
Pegasus 1	65009 A	93.8	31 7
GREB	65016 A	103.4	70.0
Gravity Gradient 2	65016 B	103.4	70 0
Gravity Gradient 3	65016 C	103.4	70.0
Solarad	65016 D	103.4	70.0
EGRS 3	65016 E	103.4	70.0
Oscar 3	65016 F	103.3	70.0
Surcal	65016 G	101.9	70.0
Dodechedron	65016 H	103.4	70.0
Explorer 27	65032 A	107.8	41.1
Pegasus 2	65039 A	95.2	31.7
Tiros 10	65051 A	100.5	98.1
OGO 2	65081 A	100.5	87.3
Explorer 30	65093 A	100.6	59.7
ESSA 1	66008 A	101.1	97.8
OAO 1	66031 A	100.8	35.0

Table VI (continued)

U.S. Satellites Within the Shuttle Retrieval Envelope (11)

Name	International Designation	Period (min)	Inclination (deg)
OV1-10	66111 B	98.5	93.4
OSO 3	67020 A	94.8	32.8
Gravity Gradient 4	67053 C	103.3	69.9
Gravity Gradient 5	67053 D	103.3	69 9
OV1-12	67072 D	94.4	101.6
OSO 4	67100 A	95.0	32.9
Explorer 37	68017 A	97.8	59.3
TETR 2	68100 B	95.0	32.8
OAO-A2	68110 A	100.2	34.9
OSO 5	69006 A	95.2	32.9
OGO 6	69051 A	96.8	81.9
OSO 6	69068 A	94.4	32.9
PAC 1	69068 B	91.7	32.9
Explorer 44	71058 A	94.6	51.0
OV1-21	71067 B	100.9	87.6
TETR 4	71083 B	92.9	33.0
Explorer 46	72061 A	97.1	37.6
Copernicus	72065 A	99.6	35.0
Triac OI-1X	72069 A	100.6	90.0
Skylab 1	73027 A	93.0	50.0
Explorer 51	73101 A	90.2	67.9
OSO 8	75057 A	95 6	32.9
TIP 2	75099 A	98.8	90.3

Table VII

Foreign Satellites Within the Shuttle Retrieval Envelope (11)

Name	International Designation	Period (min)	Inclination (deg)
Alouette 1	1962 B ALPHA 1	105.4	80.4
Polyot 1	63043 A	98.7	58.8
Cosmos 58	65014 A	96.3	65.0
Cosmos 72	65053 B	94.1	56.0
Cosmos 74	65053 D	94.6	56.0
Cosmos 75	65053 E	94.7	56.0
FR-1	65101 A	99.7	75.8
Cosmos 100	65106 A	97.3	65.0
Cosmos 103	65112 A	96.4	56.0
Cosmos 108	66038 A	96.5	65.0
Cosmos 122	66057 A	96.5	64.9
Diademe 1	67011 A	103.7	39.9
Cosmos 144	67018 A	96.1	81.1
Cosmos 151	67027 A	96.7	56.0
Cosmos 156	67039 A	96.4	81.1
Cosmos 158	67045 A	100.4	74.0
Cosmos 184	67102 A	96.6	81.1
Cosmos 189	67108 A	93.0	73.9
Cosmos 192	67116 A	99.7	74.0
Cosmos 198	67127 A	103.4	65.1
Cosmos 206	68019 A	96.5	81.2
Cosmos 209	68023 A	103.1	65.3
Cosmos 220	68040 A	98.9	74 0

Table VII (continued)

Foreign Satellites Within the Shuttle Retrieval Envelope (11)

Name	International Designation	Period (min)	Inclination (deg)
Cosmos 226	68049 A	96.3	81.1
Cosmos 236	68097 A	96.5	56.0
Cosmos 248	68090 A	93.6	62.2
Cosmos 250	68095 A	92.5	73.9
Cosmos 269	69021 A	93.3	74.0
Meteor 1	69029 A	97.7	81.1
Cosmos 292	69070 A	99.8	74.0
Meteor 2	69084 A	97.4	81.2
Cosmos 304	69091 A	99.8	74.0
Cosmos 315	69107 A	93.8	74.0
Meteor 3	70019 A	95.8	81.1
Cosmos 330	70024 A	94.1	74.0
Cosmos 332	70028 A	99.9	74.0
Meteor 4	70037 A	97.9	81.2
Meteor 5	70047 A	102.0	81.2
Cosmos 358	70064 A	94.9	74.0
Cosmos 367	70079 A	104.5	65.2
Cosmos 371	70083 A	99.8	73.9
Meteor 6	70085 A	97.3	81.2
Cosmos 372	70086 A	100.7	74.0
Cosmos 373	70087 A	93.8	62.8
Cosmos 381	70102 A	104.8	74.0
Cosmos 385	70108 A	104.7	74.0

Table VII (continued)

Foreign Satellites Within the Shuttle Retrieval Envelope (11)

Name	International Designation	Period (min)	Inclination (deg)
Cosmos 387	70111 A	94.6	73.9
Cosmos 389	70113 A	97.9	81.1
Meteor 7	71003 A	97.4	81.2
Cosmos 394	71010 A	96.4	65.8
Tansei	71011 A	106.0	29.6
Cosmos 395	71013 A	94.8	74.0
Cosmos 400	71020 A	104.9	65.8
Cosmos 402	71025 A	104.9	64.9
Tournesol	71030 A	95.4	46.3
Meteor 8	71031 A	96.9	81.2
Cosmos 407	71035 A	100.9	74.0
Cosmos 422	71046 A	105.0	74.0
Cosmos 425	71050 A	94.6	74.0
Meteor 9	71059 A	97.1	81.1
EOLE 1	71071 A	100.6	50.1
Cosmos 436	71074 A	94.6	74 0
Cosmos 437	71075 A	94.8	74.0
Prespero	71093 A	106.3	82.0
Cosmos 460	71103 A	94.7	73.9
Cosmos 461	71105 A	93.7	69.2
Ariel 4	71109 A	94.1	82.9
Cosmos 465	71111 A	104.8	74.0
Cosmos 468	71114 A	100.7	74.0

Table VII (continued)

Foreign Satellites Within the Shuttle Retrieval Envelope (11)

Name	International Designation	Period (min)	Inclination (deg)
Cosmos 469	71117 A	104.7	64 4
Meteor 10	71120 A	102.6	81.2
Cosmos 475	72009 A	104.7	74.0
Cosmos 476	72011 A	97.1	81.2
TD-1A	72014 A	95.0	97.5
Cosmos 479	72017 A	94.7	74.0
Meteor 11	72022 A	102.5	81.2
Cosmos 489	72035 A	104.7	74.0
Cosmos 494	72043 A	100.7	74.0
Meteor 12	72049 A	102.8	81.2
Cosmos 500	72053 A	94.8	74.0
Cosmos 514	72062 A	104.3	82.9
Cosmos 516	72066 A	104.5	64.8
Cosmos 521	72074 A	104.9	65.8
Meteor 13	72085 A	102.5	81.2
Cosmos 536	72088 A	94.9	74.0
Cosmos 540	72104 A	100.7	74.0
Cosmos 542	72106 A	96.2	81.2
Cosmos 544	73003 A	94.9	74.0
Cosmos 546	73005 A	96.5	50.6
Cosmos 549	73010 A	94.9	74.0
Meteor 14	73015 A	102.5	81.2
Meteor 15	73034 A	102.4	81.2

Table VII (continued)

Foreign Satellites Within the Shuttle Retrieval Envelope (11)

Name	International Designation	Period (min)	Inclination (deg)
Cosmos 574	73042 A	105.0	82.9
Cosmos 582	73060 A	95.0	74 0
Cosmos 586	73065 A	104.8	82.9
Cosmos 604	73080 A	97.1	81.2
Intercosmos 10	73082 A	95.2	73.9
Cosmos 610	73093 A	95.0	74.0
Cosmos 614	73098 A	100.6	74.0
Cosmos 626	73108 A	104.0	65.4
Cosmos 627	73109 A	105.0	82.9
Cosmos 628	74001 A	104.8	82.9
Cosmos 631	74005 A	95.1	74.0
Meteor 16	74011 A	102.1	81.2
UK-X4	74013 A	101.1	97.8
Cosmos 648	74024 H	102.5	81.2
Cosmos 651	74029 A	103.4	64.9
Cosmos 654	74032 A	104.4	64.9
Intercosmos 11	74034 A	94.5	50 5
Cosmos 655	74035 A	95.1	74.0
Cosmos 661	74045 A	95.0	74.0
Cosmos 662	74047 A	90.5	70.8
Cosmos 663	74048 A	104.8	82.9
Meteor 18	74052 A	103.0	81.2
Cosmos 673	74066 A	97.0	81.2

Table VII (continued)

Foreign Satellites Within the Shuttle Retrieval Envelope (11)

Name	International Designation	Period (min)	Inclination (deg)
ANS	74070 A	94.9	98.0
Cosmos 676	74071 A	100.9	74.0
Cosmos 687	74076 A	93.0	73.9
Cosmos 689	74079 A	105.0	82.9
Meteor 19	74083 A	102.4	81.1
Meteor 20	74099 A	102.3	81.2
Cosmos 698	74100 A	95.2	74.0
Cosmos 700	74105 A	104.7	82.9
Salyut 4	74104 A	90.9	51.5
Cosmos 699	74103 A	92.6	65.0
Cosmos 707	75008 A	95.0	74.0
Starlette	75010 A	104.1	49.8
Intercosmos 13	75022 A	103.9	82.9
Meteor 21	75023 A	102.5	81.2
Cosmos 723	75024 A	103.7	64.7
Cosmos 724	75025 A	103.0	65.5
Cosmos 726	75028 A	104.6	82.9
Ariabat	75033 A	96.4	50.6
Cosmos 729	75034 A	104.9	82.9
Castor	75039 B	99.0	29.9
Cosmos 744	75056 A	97.0	81.2
Cosmos 749	75062 A	95.1	74.0
Meteor 2	75064 A	102.4	81.2

Table VII (continued)

Foreign Satellites Within the Shuttle Retrieval Envelope (11)

Name	International Designation	Period (min)	Inclination (deg)
Cosmos 750	75067 A	93.9	71.0
Cosmos 752	75069 A	94.5	65.8
Cosmos 755	75074 A	104.9	82.9
Cosmos 756	75076 A	97 2	81.2
KIKU	75082 A	105.9	46.9
Meteor 22	75087 A	102.3	81.2
D2-B	75092 A	96.8	37.1
Cosmos 773	75094 A	100.8	74.0
Cosmos 778	75103 A	104.8	82.9
Cosmos 781	75109 A	95.1	74.0
Cosmos 783	75112 A	100.9	74.0
Intercosmos 14	75115 A	105.1	73.9
Cosmos 785	75116 A	104.2	65.0
Meteor 23	75124 A	102.3	81.2
Cosmos 787	76001 A	95.2	74.0
Cosmos 789	76005 A	104.9	82.9
Cosmos 790	76007 A	95.2	74.0
Cosmos 800	76011 A	105.0	82.9
Cosmos 801	76012 A	94.7	70.9
Cosmos 803	76014 A	96.3	65.8
UME	76019 A	105.1	69.6
Cosmos 808	76024 A	97.0	81.2
Cosmos 812	76031 A	95.1	74.0

Table VII (continued)

Foreign Satellites Within the Shuttle Retrieval Envelope (11)

Name	International Designation	Period (min)	Inclination (deg)
Meteor 24	76032 A	102.2	81.2
Cosmos 816	76037 A	94.5	65.8
Meteor 25	76043 A	102.3	81.2
Cosmos 818	76044 A	91.8	71.0
Cosmos 822	76049 A	94.4	74.0
Cosmos 823	76051 A	104.9	82.9
Intercosmos 15	76056 A	94.6	74.0
Salyut 5	76057 A	89.2	51.5
Cosmos 834	76058 A	88.9	81.3
Cosmos 835	76060 A	100.9	74.0
Cosmos 836	76061 A	89.4	65.0